Evolution of Damped Lyman α Systems from Hierarchical Structure Formation Models

Katsuya Okoshi (The University of Electro-communications)

Okoshi, Nagashima, Gouda and Yoshioka 2004 ApJ, 603,12
Okoshi and Nagashima 2005 ApJ, 623,99
Okoshi,Nagashima and Gouda 2006 submitted to ApJ

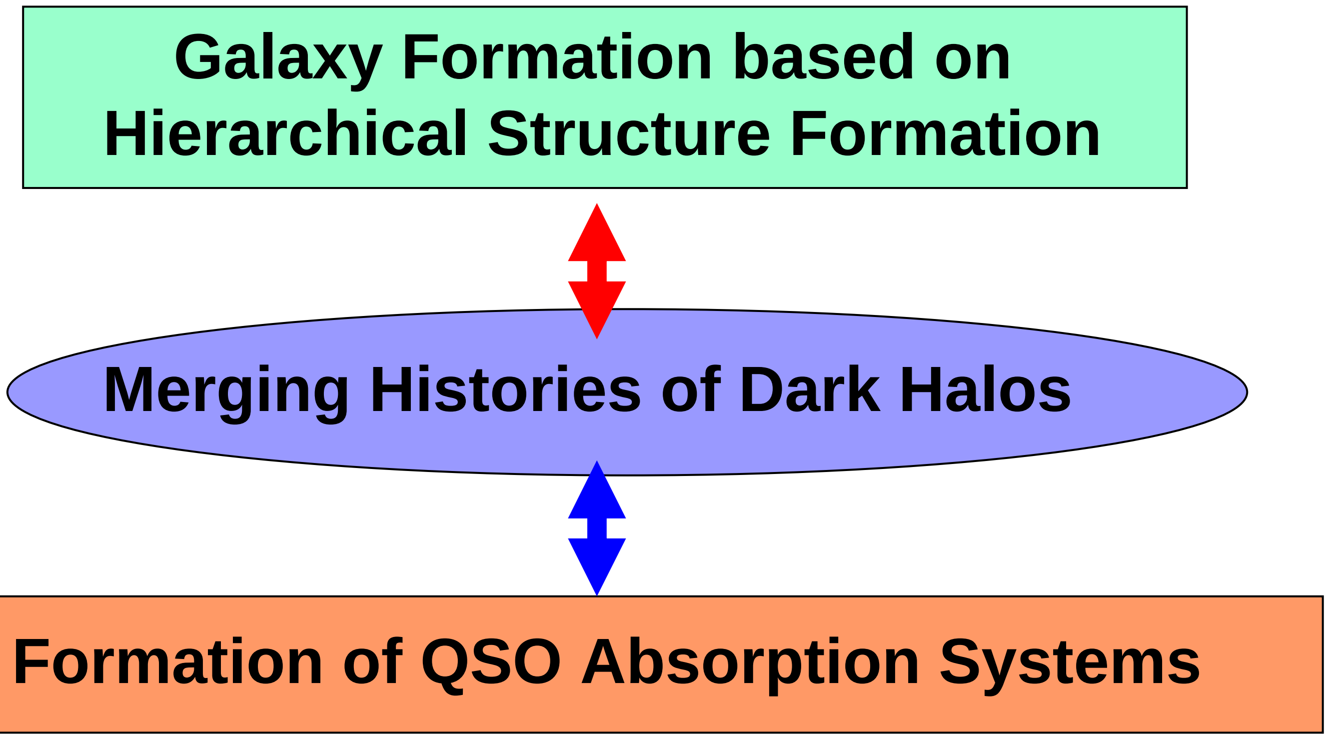

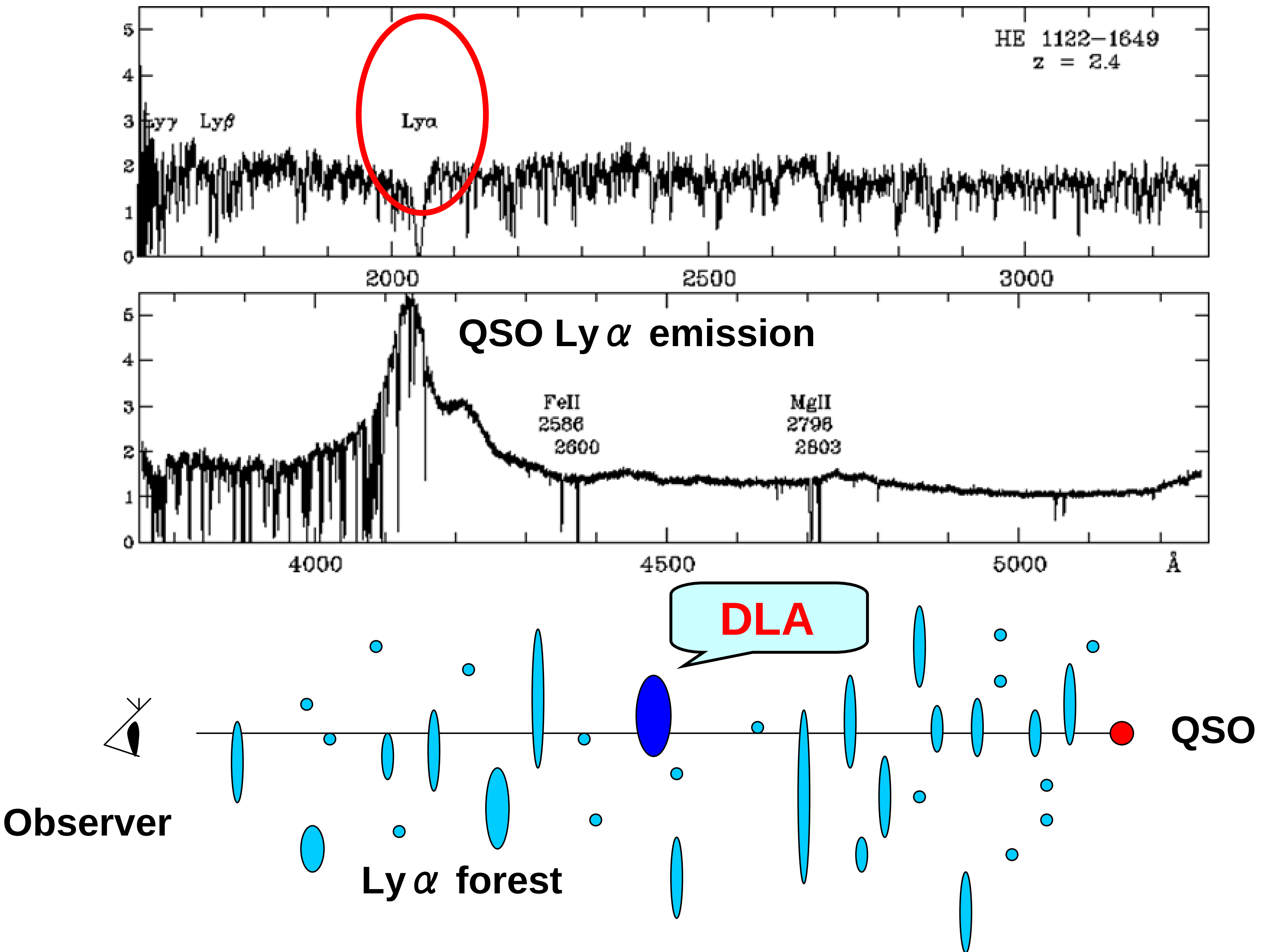
HE 1122−1649
z = 2.4
Lyγ
Lyβ
Lyα
2000
2500
3000
QSO Lyα emission
FeII
2586
2600
MgII
2796
2803
4000
4500
5000
Å
DLA
QSO
Observer
Lyα forest

QSO Absorption Systems

Types	redshift	Log N(HI)	Origin
Ly α cloud	0-4.5	13-17	Intergalactic cloud or/and galactic gas
LLS	1-4.0	17-20	？？？
DLA	0-4.5	20-22	galactic disk gas（?）
C IV	1-3.5	--------	halo hot gas (10^5 K)
Mg II	0-2.2	--------	halo warm gas (10^3 K)

1．Introduction
なぜDLA Systemに注目するのか？

1. **High HI column density system** $N_{HI} > 10^{20.3}\ cm^{-2}$

→ Optically Thick (!) Systems $N_{HI} > 10^{17}\ cm^{-2}$

→ ***Star Formation Process の解明***

(cf. Surface density in the disk of the Milky Way;
$N_{gas} = 55 \pm 10\ M_{\odot} pc^{-2} = 10^{21.8}\ cm^{-2}$)

2. **More abundant systems at high redshift**

→ *多数のシステムが見つかりやすい（Typical L*-galaxy の10倍以上）*

3. **Precise measurements of metal abundance in GAS (not STAR)**

Mild metallicity evolution (0 <z< 4.5)

DLAの個数密度

典型的な(massive spiral)銀河と比較すると・・・

$$\left(\frac{dN}{dz}\right)_{\substack{\text{typical}\\\text{galaxy}}} = \Phi_{g,0}(1+z)^3 \pi R_g^2 \frac{c}{H_0 \Omega^{1/2}(1+z)^{5/2}} \approx 0.02\Omega^{1/2}$$

$$(z = 3; \Phi_{g,0} = 0.01 h^3 \mathrm{Mpc}^{-3}, R_g = 10 h^{-1} \mathrm{kpc})$$

$$\Rightarrow \left(\frac{dN}{dz}\right)_{\mathrm{DLA}} \approx 10 \left(\frac{dN}{dz}\right)_{\substack{\text{typical}\\\text{galaxy}}}$$

Redshift Distribution

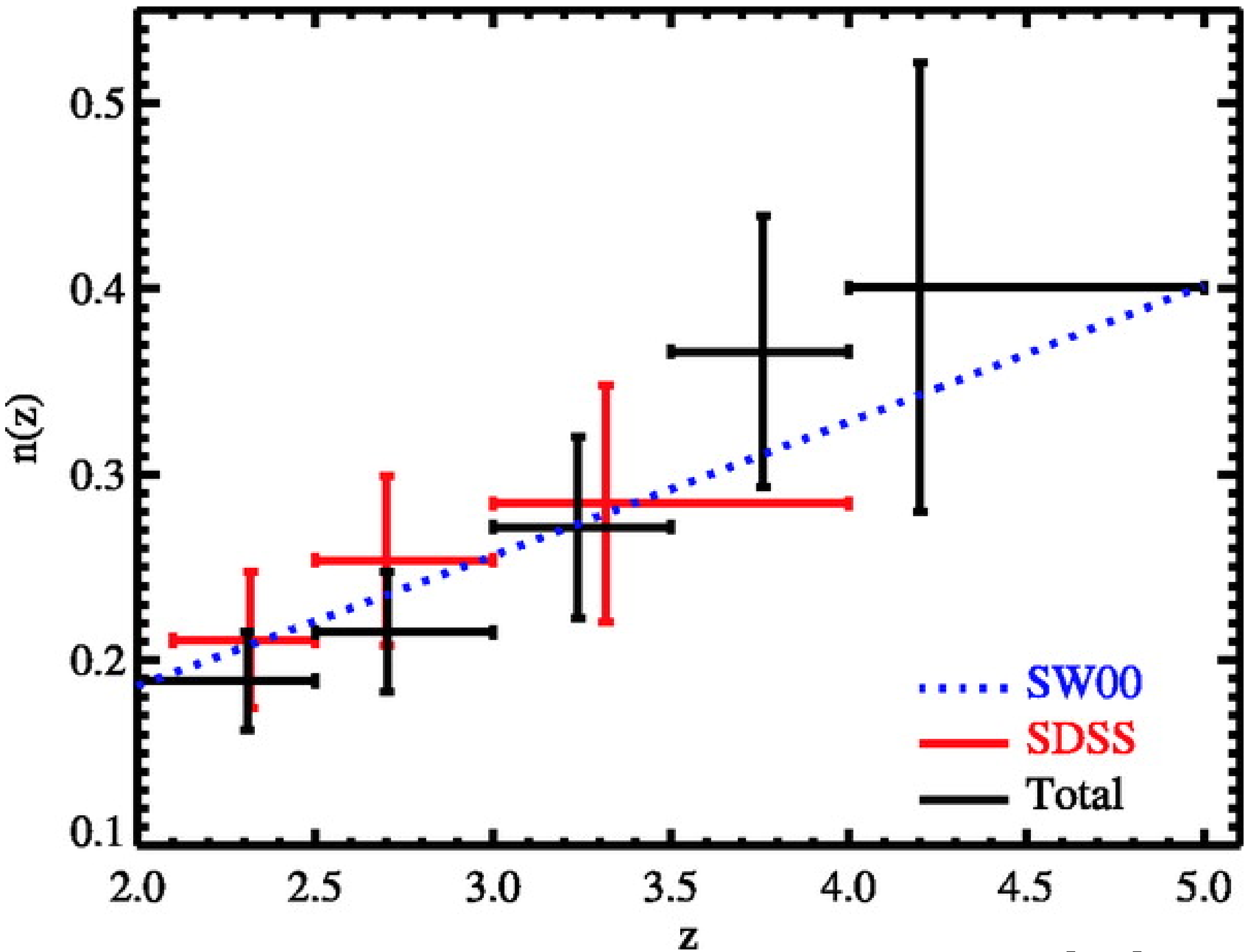

Prochaska et al. 2004

3. Precise measurements of metal abundance in GAS (not STAR)

125 DLAsからGas Metallcityを測定

Mild metallicity evolution (0 <z< 4.5）
(e.g., Prochaska et al.2003)

4. Dust-poor system (cf typical galaxy)

***Small amount* of dust (e.g. E(B-V)<0.01: Murphy & Liske 2004)**
***No evidence* for a statistically significant *dust bias* in MgII-selected DLA surveys at 0.5 < z(abs) <3.5**
(Ellison et al. 2001, 2004)

>> 'Unbiased' Tracer : Metallicity Evolution of Pre-galactic System

>> Stringent Constraints on Galaxy Formation

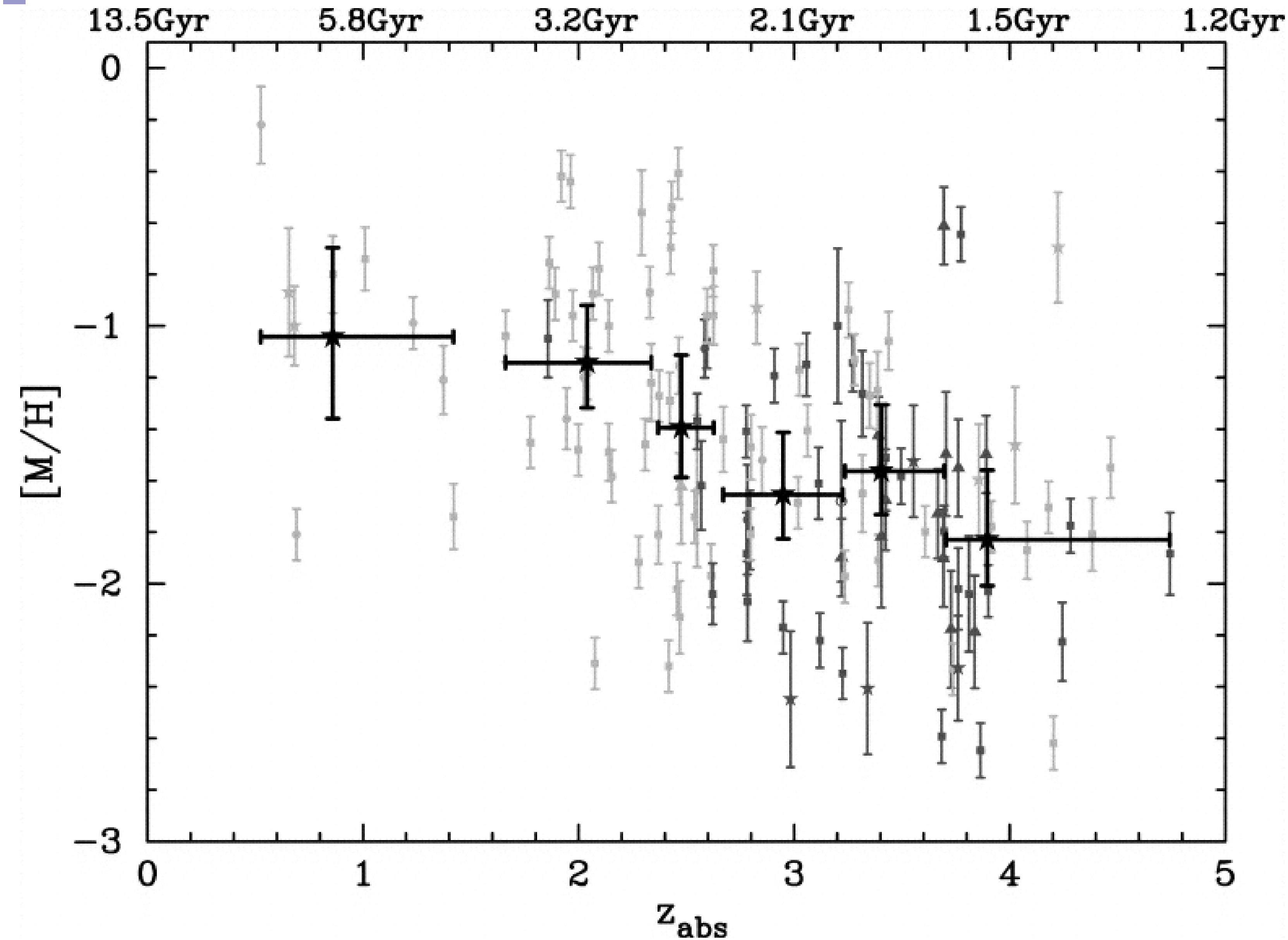

Prochaska et al. 2003

5. HI ガスの貯蔵庫

DLA contains a significant fraction of the HI gas in the universe!

Ω(HI) ~ 10^-3 at 0 < z < 4

$$\Omega_{\rm DLA} \propto \int N_{\rm HI} \frac{\partial^2 N}{\partial N_{\rm HI} \partial z} dN_{\rm HI}$$

$$\frac{dN}{dN_{\rm HI}} \propto N_{\rm HI}^{-\beta}$$

(β =1.4-1.6; Rao et al. 2005; Prochaska et al. 2004)

$$\Omega_{\rm DLA} \propto \int N_{\rm HI} N_{\rm HI}^{-\beta} dN_{\rm HI} \propto \int N_{\rm HI}^{1-\beta} dN_{\rm HI}$$

$$\propto [N_{\rm HI}^{2-\beta}]^{N_{\rm HI}(max)} \sim N_{\rm HI}(max)^{2-\beta}$$

→ ***HI ガスのほとんどが、DLAに存在している！***

Gas Density

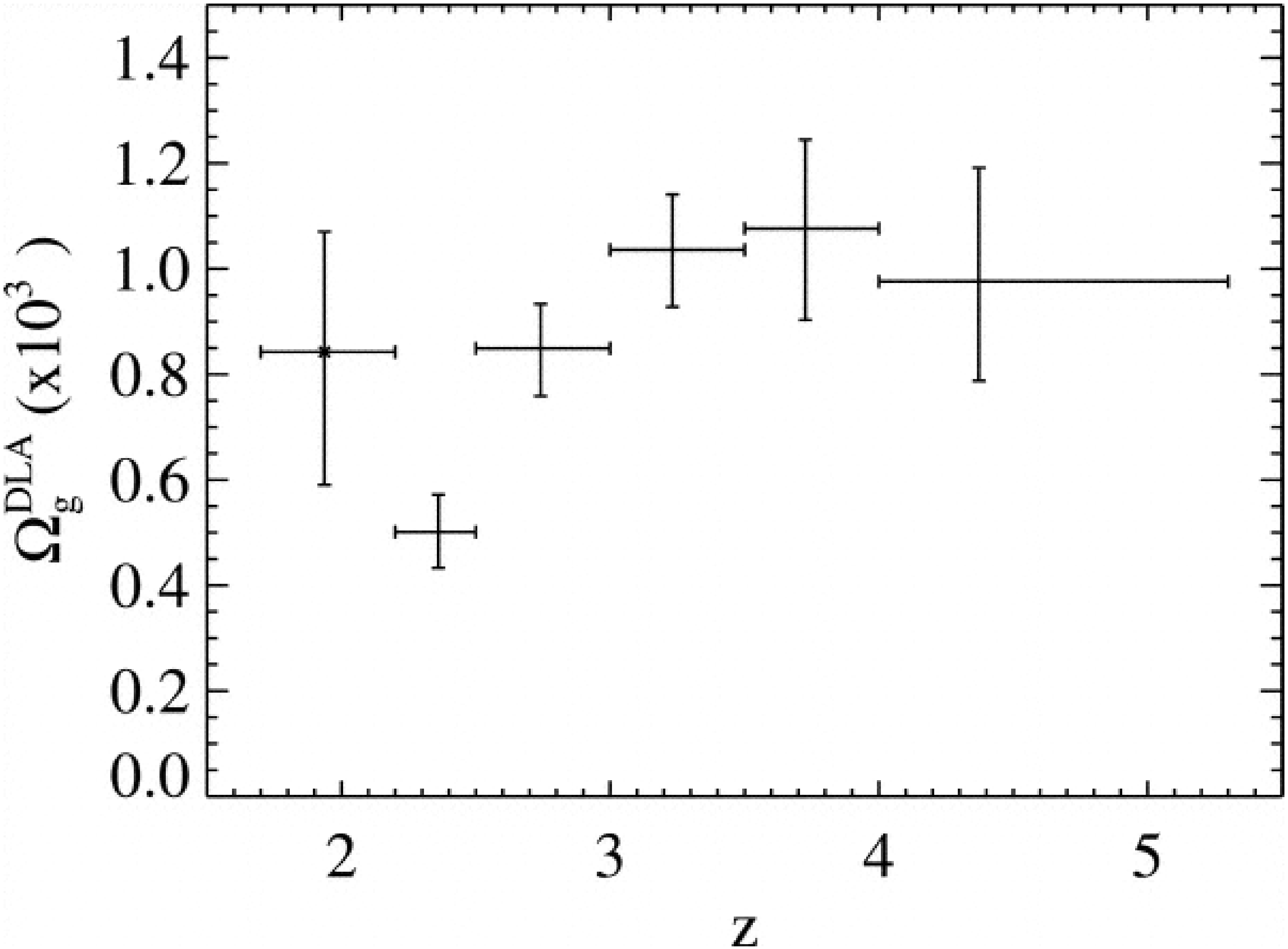

Prochaska et al. 2005

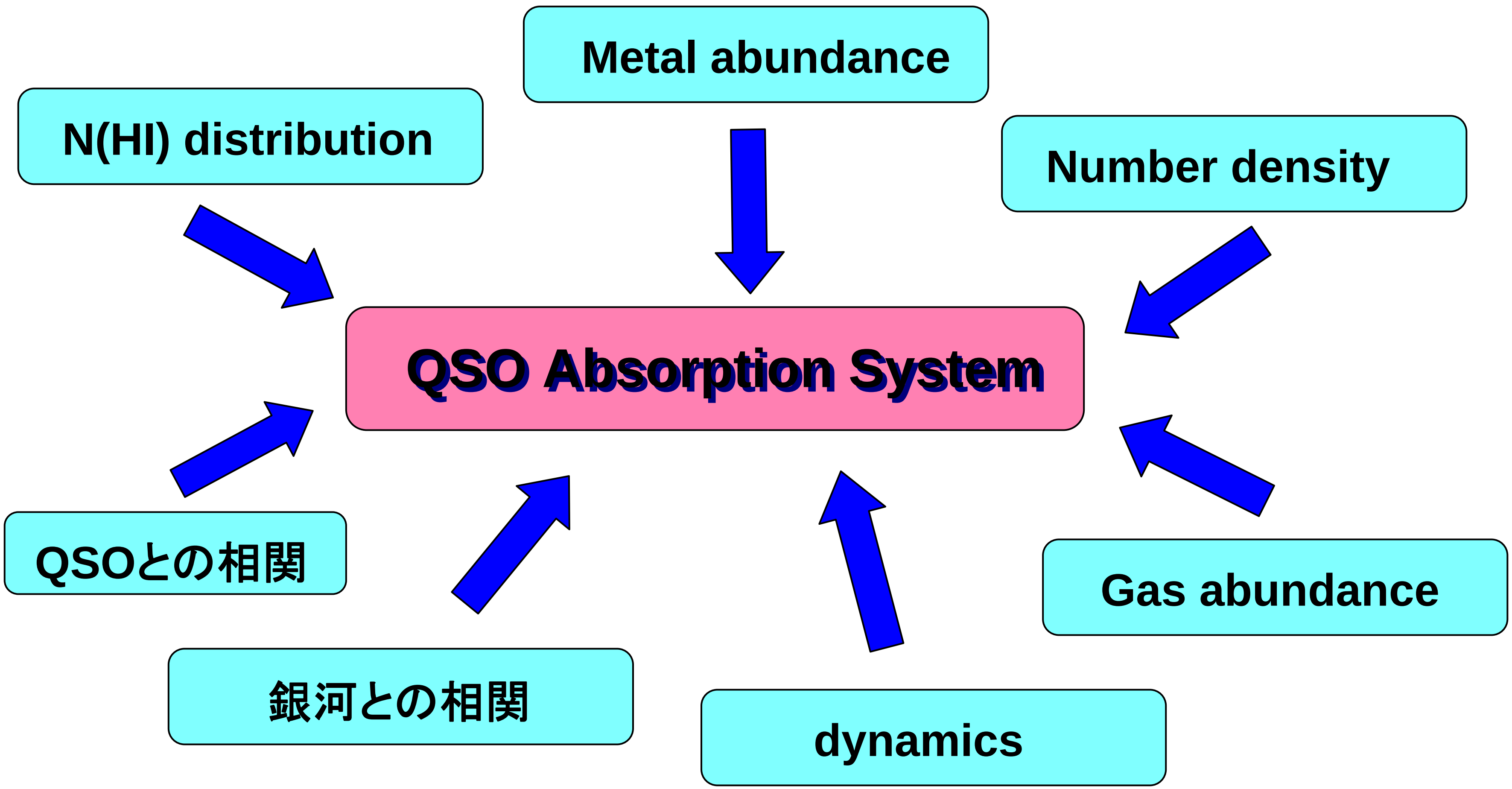

Metal abundance
N(HI) distribution
Number density
QSO Absorption System
QSOとの相関
Gas abundance
銀河との相関
dynamics

Semi-Analytic Approach to Structure Formation

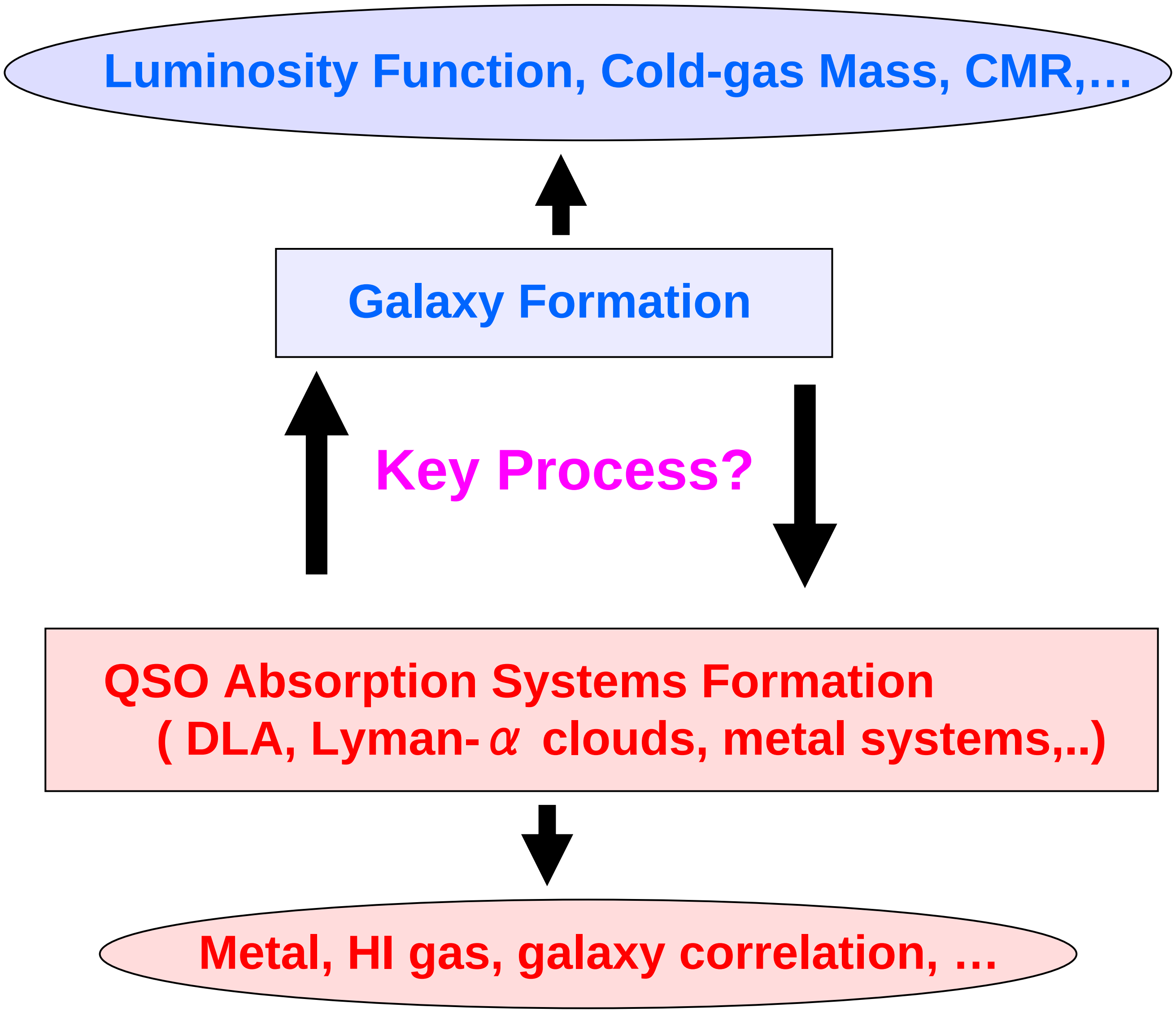

2. Model

Dark HalosのMerging **Process**

Probability Function f(M,z | M',z')dM:
Halo (mass M' redshift z') has a progenitor (M,z)

>> Press-Schechter Mass Function n(M,z | M',z')

Dark halos

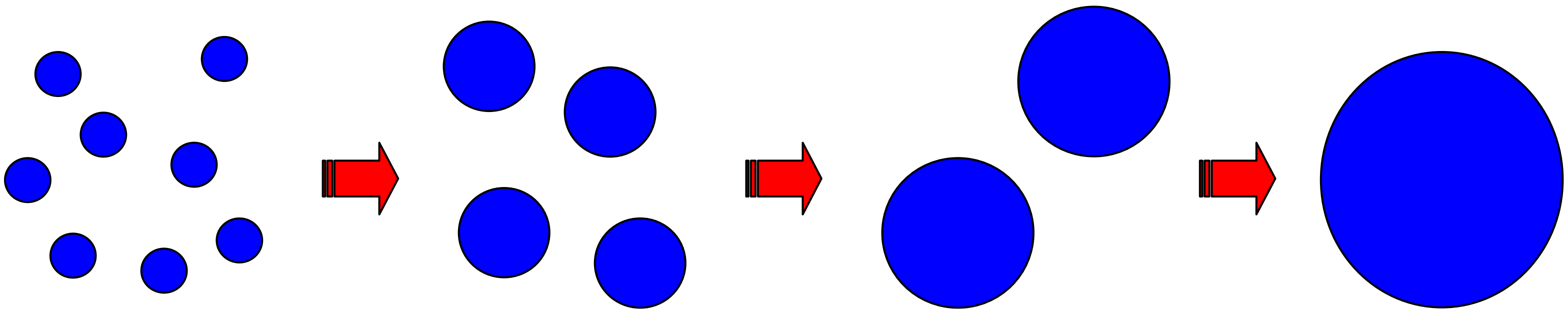

Density perturbations

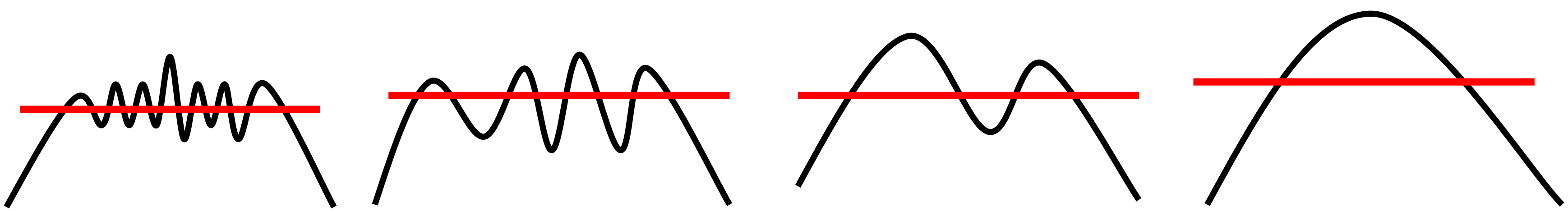

ガスの進化過程について

(A) Life time

Life time of halo is equal to cooing time of gas

$$\mathbf{t}_{\text{life}} = \tau_{\text{cool}}(\mathbf{r}_{\text{cool}}) = \frac{2}{3}\frac{\rho_{\text{gas}}\mathbf{r}_{\text{cool}}}{\mu \mathbf{m}_{\text{p}}}\frac{\mathbf{kT}}{\mathbf{n}_{\text{e}}^{2}\mathbf{r}_{\text{cool}}\Lambda(\mathbf{T})} \quad (\rho_{\text{gas}}(\mathbf{r}) \propto \mathbf{n}_{\text{e}}(\mathbf{r}) \propto \mathbf{r}^{-2})$$

(B) Star Formation Process

$$\dot{\mathbf{M}}_{*} = \frac{\mathbf{M}_{\text{cold}}}{\tau_{*}}$$

$$\tau_{*} = \tau_{*}^{0}\left(\frac{\mathbf{V}_{\text{c}}}{300\ \mathbf{km}/\mathbf{s}}\right)^{\alpha_{*}}(1+\mathbf{z})^{\alpha_{\text{z}}}$$

$\alpha_z = -1.5(\propto t_{dyn})$ **:accelerated efficiency model**

0 : constant efficiency model

$$\tau_{*}^{0} \cong 2-5\,\mathbf{Gyr}\,(\mathbf{M}/\mathbf{L}_{\mathbf{B}} - \mathbf{V}_{\mathbf{c}}\,\mathbf{relation})$$

→ $\tau_{*}^{0}, \alpha_{*}, \alpha_{\text{z}}$

(C) Supernovae Feedback

Energy input by SN explosions

$$\frac{dM_{rehaeat}}{dt} = \varepsilon \frac{4}{5} \frac{\eta_{SN} E_{SN}}{V_c^2} \dot{M}_* \left(= \beta \dot{M}_* \right)$$

$$\beta(V_c) = \left(\frac{V_c}{V_{hot}} \right)^{-\alpha_{hot}}$$

ε : input efficiency

η_{SN} : fraction of stars $M \geq 8M_\Theta$

E_{SN} : energy release per a SN $(=10^{51} erg)$

α_{hot} : $\alpha_{hot} = 2$

(D) Population Synthesis

Total Luminosity

$$L_* = \int \dot{M}_* Z_{cold} dt$$

Stellar population synthesis model

(F) Chemical Evolution

Basic Equation for 2 phase model (Cold and Hot gas components)

$$\frac{dM_c}{dt} = -\dot{M}_* + F(t)(1-f) + g(t) - \beta \dot{M}_*$$

$$\frac{dM_*}{dt} = \frac{M_c}{\tau_*}$$

$$\frac{dM_h}{dt} = \beta \dot{M}_* - g(t) + F(t)f + A(t)$$

$$g(t) = 4\pi\rho_h(r_{cool})r_{cool}^2 \frac{dr_{cool}}{dt} \cong \frac{M_c^0}{\tau}$$

$$\frac{dM_cZ_c}{dt} = (1-f)(F_Z(t) + R_Z(t)) - Z_c\dot{M}_* + Z_h g(t) - Z_c\beta\dot{M}_*$$

$$\frac{dM_hZ_h}{dt} = f(F_Z(t) + R_Z(t)) + Z_c\beta\dot{M}_* - Z_h g(t) + Z_d A(t)$$

β : **SN feedback** **g: cooling gas inflow**

F: gas inflow from stars Fz: metal mass produced by new stars
Rz: metal mass inflow A: gas mass accreted from diffuse matter(=0)

Here we apply 'Instantaneous Recyclic Approximation'.

銀河のMerging Processes

Dark halosのmerging process

↓

Hot gas は新しくできた一つのhaloの中で共有する。

最もmassiveな銀河を’central galaxy’とし、それ以外の銀河を‘satellites’と呼ぶ。
このとき、これらの銀河どうしがmergeする。

↓

Criteria for merging processes of galaxies

Satellite-Central merger : t (elapse) > t (dynamical friction)
Satellite-Satellite merger: t > t (random collision)

Type of merging processes (satellites v central galaxy)

Two types: Major and Minor merge

Major merge

$$m_{small} / m_{large} > f_{bulge}$$

> Star burst, Bulge formation (all stars reside in central bulge)

Minor merge

$$m_{small} / m_{large} < f_{bulge}$$

> Disk formation (stars in satellites >> disk components)

Reference Models

standard models in galaxy formation model

$(\Omega_0, \Omega_\Lambda, h, \sigma_8)$

LCDM	(0.3, 0.7, 0.7, 1)

$(V_{hot}\,(km/s), \alpha_{hot}, \tau^0_*, \alpha_*)$

LC	(280,	2.5,	1.5,	-2)	(Reference Model)
LD	(280,	2.5,	4,	-2)	

Astrophysical parameters are given by as follows:

1. Galaxy luminosity function (B- and K- bands)

$$\alpha_{hot}, V_{hot}$$

(<< SN feedback process)

2. Cold-gas mass fraction

$$\alpha_*, \tau_*^0$$

すべて local galaxyに関する観測量で決める

DLAの同定

1. **HI Central column density**

$$N_{\rm HI}(0) = \frac{M_{\rm HI}(r=0)}{\pi r_d^2}$$

2. **Inclination of gaseous disks**

$$N_{\rm HI,c} = \frac{N_{\rm HI}(0)}{\mu} \quad (\mu = \cos\theta : inclination)$$

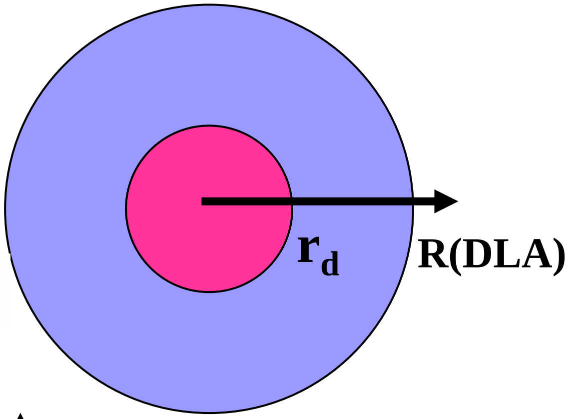

3.Disk size

Exponential profile

$$N_{\rm HI}(r) = N_{\rm HI,c}\exp(-r/r_{\rm d})$$

R(DLA) = r(N_{HI}=$10^{20.3}$ cm^{-2})

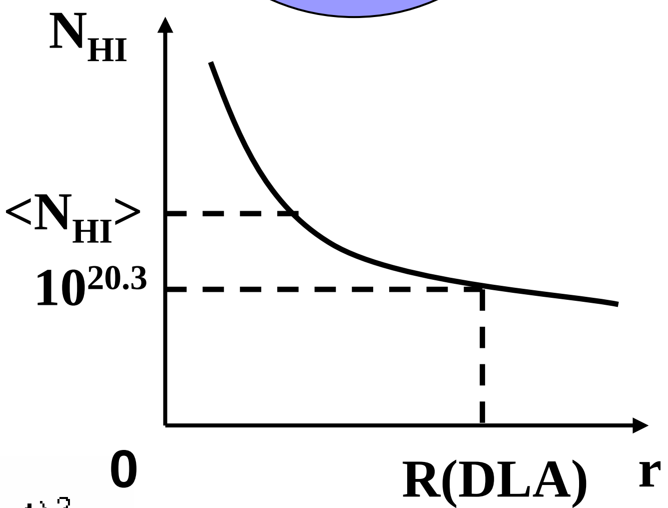

4. Average of HI column density

$$< N_{\rm HI} >= \int_0^{R(DLA)} N_{\rm HI}(r)d(\pi r^2)/\pi R(DLA)^2$$

§ 3. RESULTS

[A] *GLOBAL PROPERTIES OF DLA SYSTEMS*

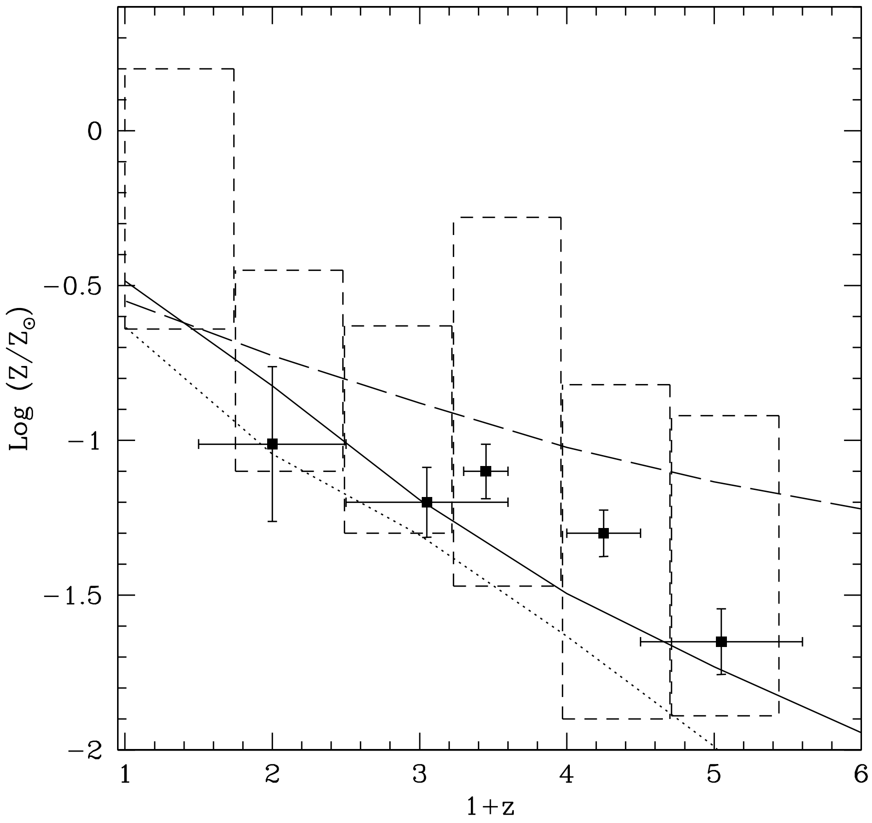

Metallicity of cold gas in DLA systems

solid line: Our best model
dotted line: stellar metallicity
dashed line: a model with $\tau_*\propto$dynamical timescale of disks (LD model)
observational data: Prochaska and Wolfe 2000, Savaglio 2001

・The metallicity shows mild evolution.
・The star formation timescale should be nearly constant

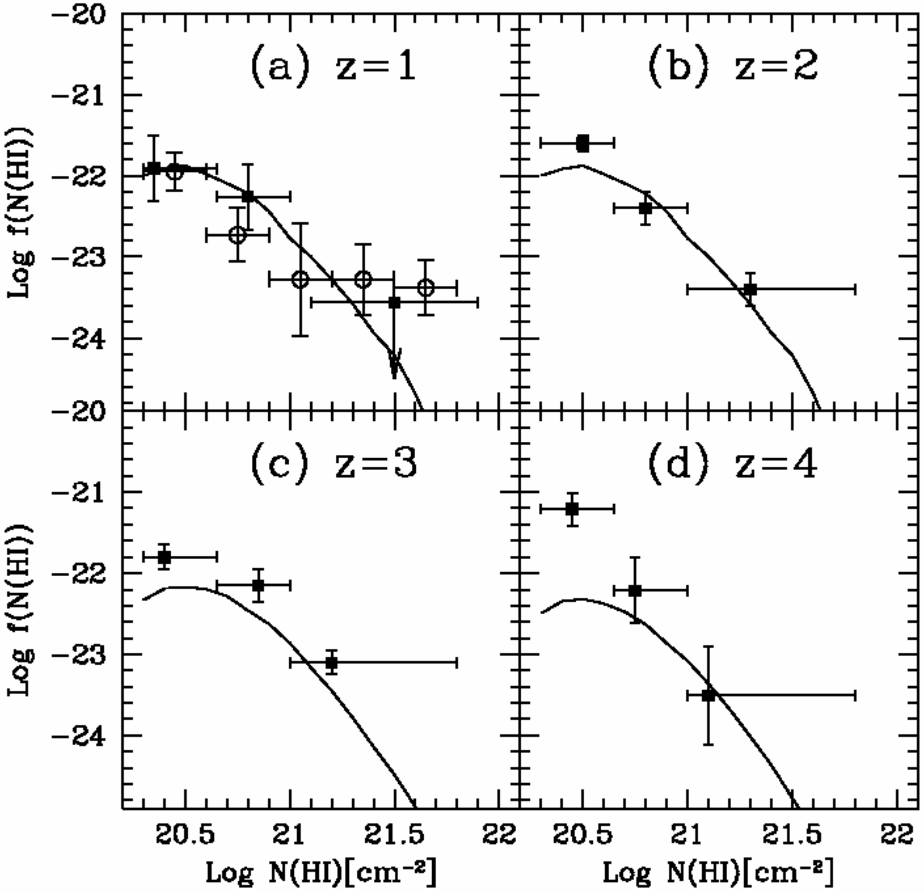

HI column density distribution

solid line: Our best model
observational data:
Prochaska and Wolfe 2000

- **Our model reproduces the HI column density distribution.**

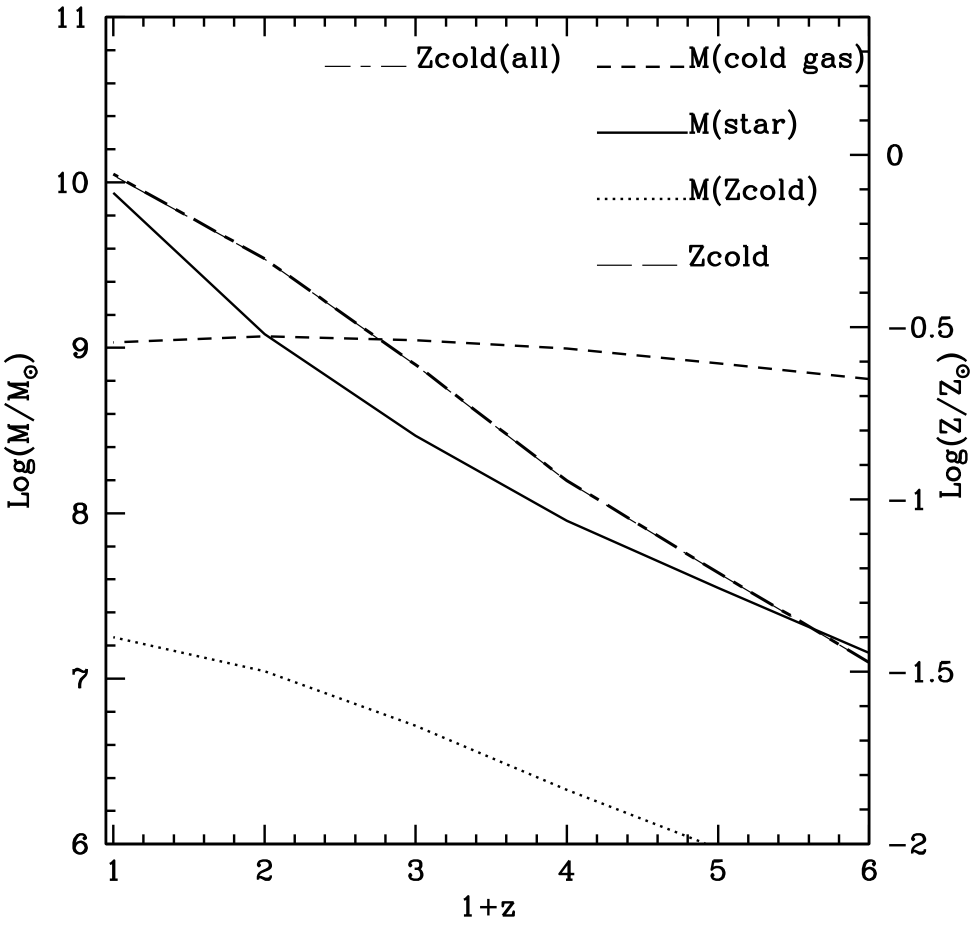

Average mass evolution of each phase:

cold gas (dashed line), stars(soild line), metals(dotted line)

Metallicity weighted by mass

cold gas in DLAs (long-dashed line)
cold gas in all galaxies (dot-dahed line)

- The average HI mass M(HI) is ~$10^9 M_\odot$
- Chemical enrichment in DLAs is similar to that in all galaxies

論点:

■DLAのhost galaxyはどのような特徴をもつのか?

■Compact object:

galactic disk, minihalo, …?

■Diffuse gas:

filament, clump, …?

⇒ Low redshifts (0<z<1)の様々な観測的特徴に注目。

⇒ typical galaxiesと比較しながら、DLAのhost galaxyを探る。

[B] *Low-redshift DLA systems*

We focus on DLA systems at redshift 0<z<1 ⇒ What are DLA galaxies ?

・Luminosity, HI column density, size etc. ← photometric counterparts

(e.g. Rao et al.2003, Rao 2005 Proceedings of IAU conference No.199)

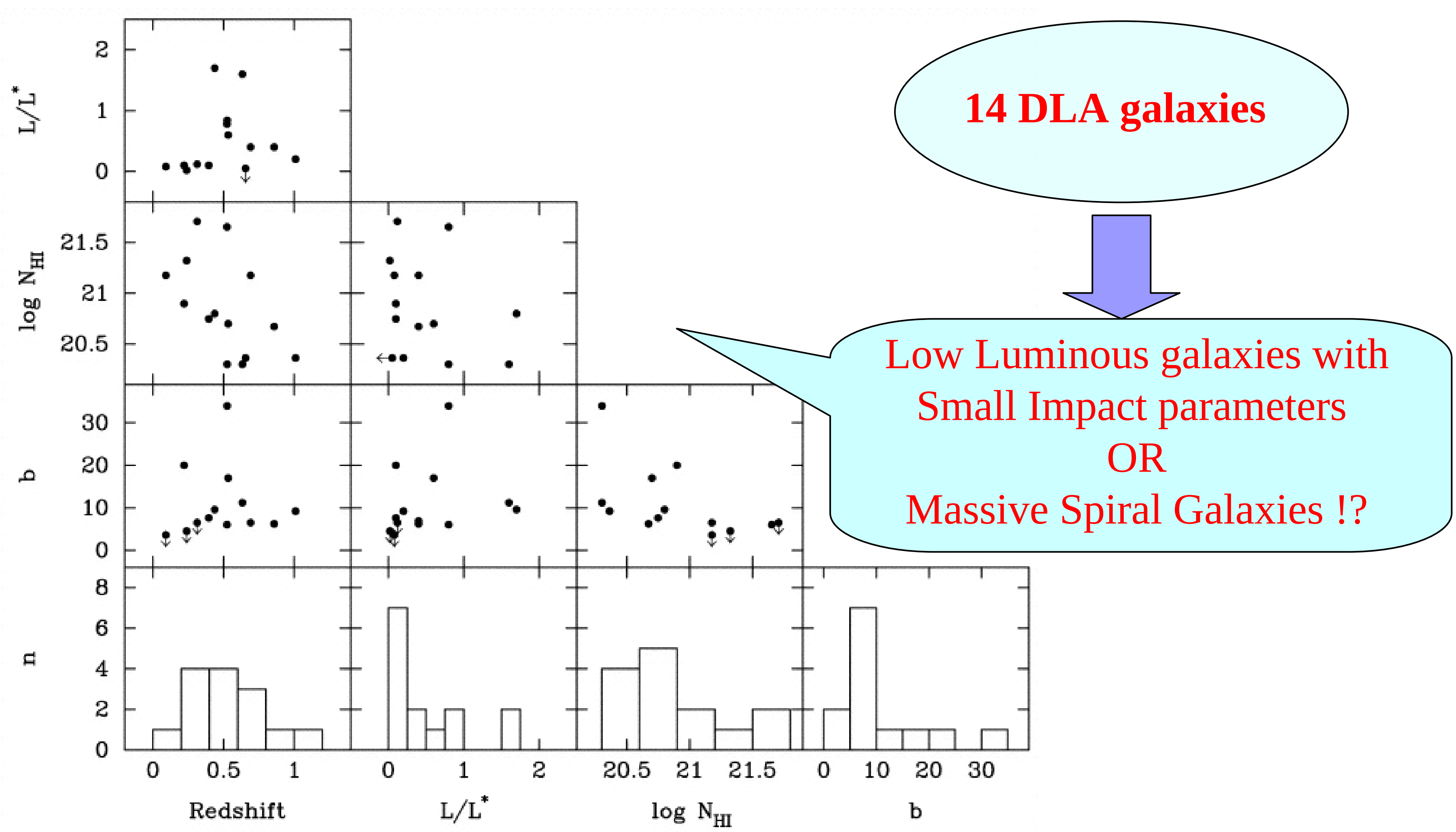

TABLE 4

Low-Redshift DLA Galaxy Properties

QSO	z_{DLA}	$N_{HI}/10^{20}$ (atoms cm^{-2})	Luminosity[a]	b (kpc)	Morphology	Reference
This Work						
B2 0827+243	0.525	2.0	$0.8L_B^*$, $1.6L_R^*$, $1.2L_K^*$	34	Disturbed spiral	1
PKS 0952+179	0.239	21	$0.02L_K^*$[b]	<4.5	Dwarf LSB	1
PKS 1127−145	0.313	51	$0.12L_B^*$, $0.16L_R^*$, $0.04L_K^*$[c]	<6.5	Patchy/irr/LSB	1
PKS 1629+120	0.532	5.0	$0.6L_B^*$, $1.1L_R^*$, $0.6L_K^*$	17	Spiral	1
Other Work						
AO 0235+164	0.524	45[e]	$0.8L_B^*$	6.0	Late-type spiral[e]	2, 3
EX 0302−223	1.010	2.3	$0.2L_B^*$	9.2	Semicompact	4
PKS 0454+039	0.859	4.7	$0.4L_B^*$	6.4	Compact	4
Q0738+313 (OI 363)	0.091	15	$0.08L_K^*$	<3.6	LSB	5
	0.221	7.9	$0.1L_B^*$	20	Dwarf spiral	5
Q0809+483 (3C 196)	0.437	6.3	$1.7L_B^*$	9.6	Giant Sbc	4
Q1209+107	0.633	2.0	$1.6L_B^*$	11.2	Spiral	4
PKS 1229−021	0.395	5.6	$0.1L_B^*$	7.6	LSB	4, 6
Q1328+307 (3C 286)	0.692	15	$0.4L_B^*$	6.5	LSB	4, 6
Q1622+239 (3C 336)	0.656	2.3	$<0.05L_K^*$	...	LSB? compact?	7

Note.—Only galaxies with cosmological redshifts are included. Thus, the DLA galaxy at $z = 0.010$, SBS 1543+593, is excluded, since it does not fall well beyond the local velocity field, which is defined at 3000 km s^{-1} by the outer boundary of the Virgo cluster (Binggeli, Popescu, & Tammann 1993). We note that it is an LSB galaxy, with $L_B = 0.02L_B^*$ and $b = 0.8$ kpc (Bowen, Tripp, & Jenkins 2001; R. E. Schulte-Ladbeck et al. 2003, in preparation).

[a] $M_B^* = -20.9$ (Marinoni et al. 1999), $M_R^* = -21.2$ (Lin et al. 1996), and $M_K^* = -24.5$ (Loveday 2000), for $q_0 = 0.5$ and $H_0 = 65$ km s^{-1} Mpc^{-1}.

[b] Sum of luminosities of objects 1 and 2 (see § 3.2.2 and Fig. 3).

[c] Sum of luminosities of objects 1, 3, and 4 (see § 3.3.1 and Fig. 4).

[d] Column density from Turnshek et al. 2003.

[e] The object defined as A1 in Yanny, York, & Gallagher 1989 and Burbidge et al. 1996 has the smallest impact parameter and, therefore, we have assumed that it is the DLA galaxy. A K-correction of 1 mag, which is appropriate for a late-type spiral galaxy at $z = 0.524$ (Poggianti 1997) has been applied to derive the absolute luminosity of A1 from the apparent magnitude measured by Burbidge et al. 1996

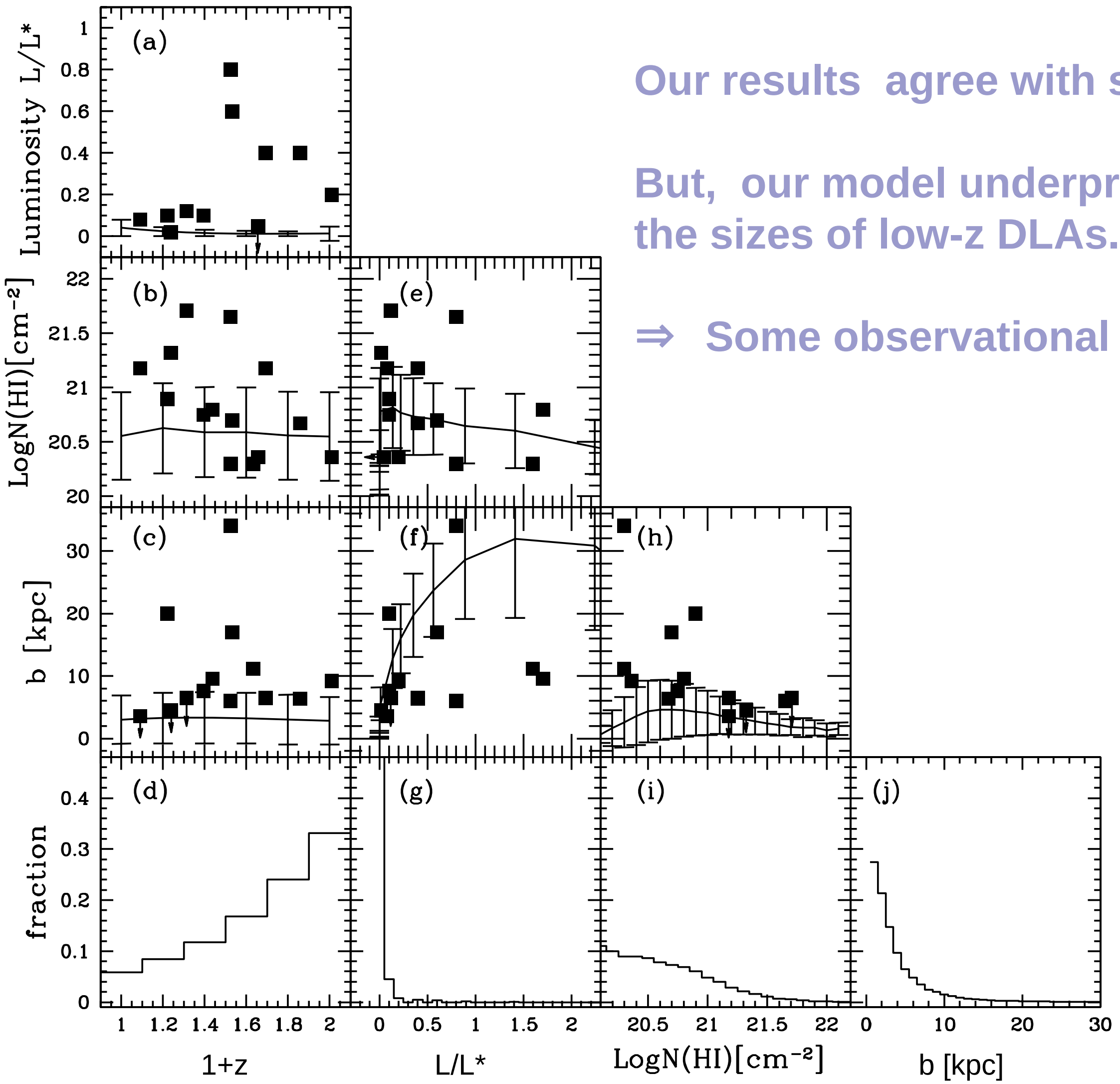

Our results agree with some observation trends.

But, our model underpredicts the luminosities and the sizes of low-z DLAs.

⇒ Some observational biases?

Next, we take into account a selection effect of DLA galaxies

(1) Surface brightness dimming effect: fail to identify DLA galaxies fainter than observational brightness limits (>25 mag arcsec^-1)

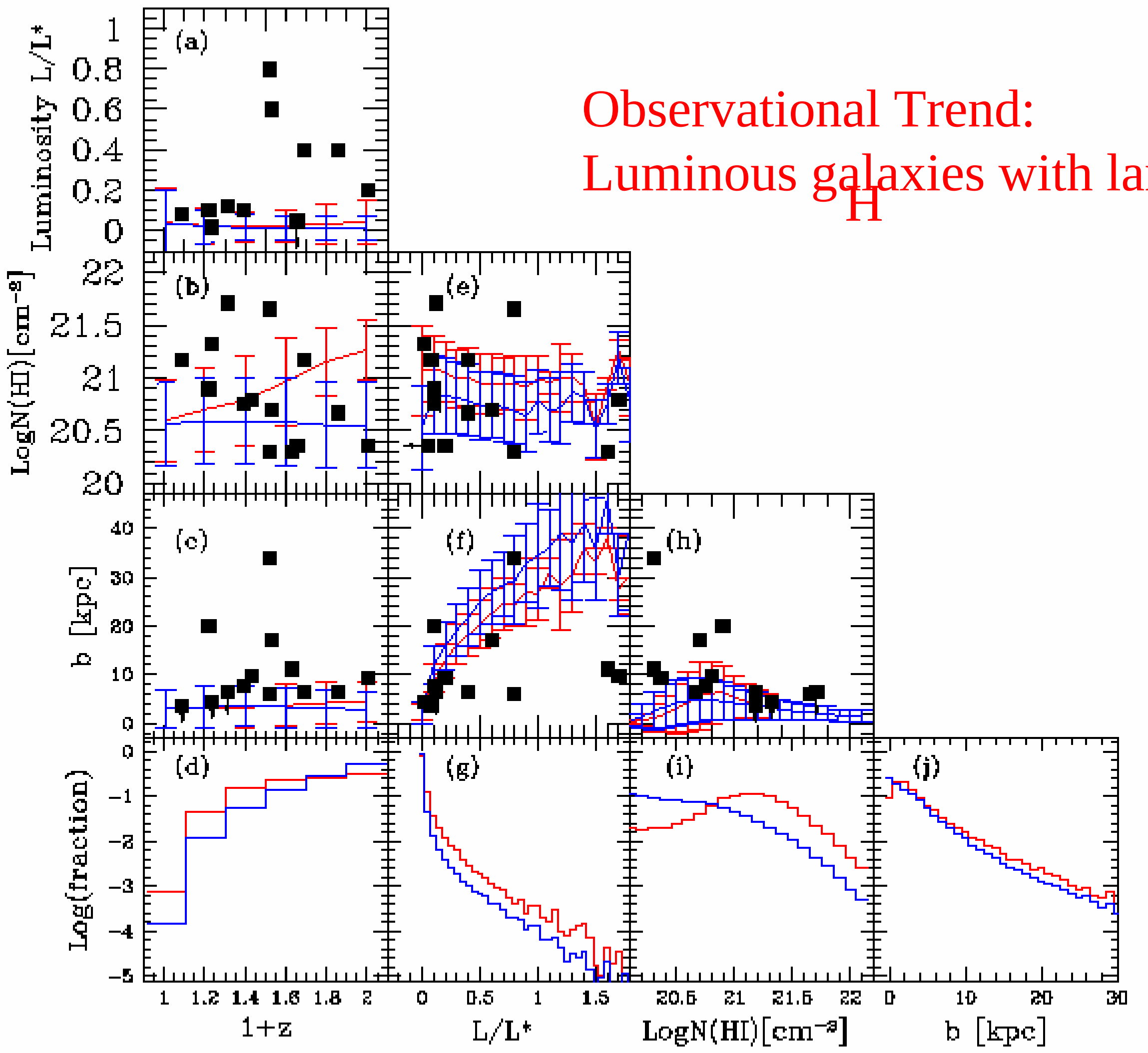

Observational Trend:

Luminous galaxies with large impact parameters ?

H

Direct Search for optical counterparts of DLAs

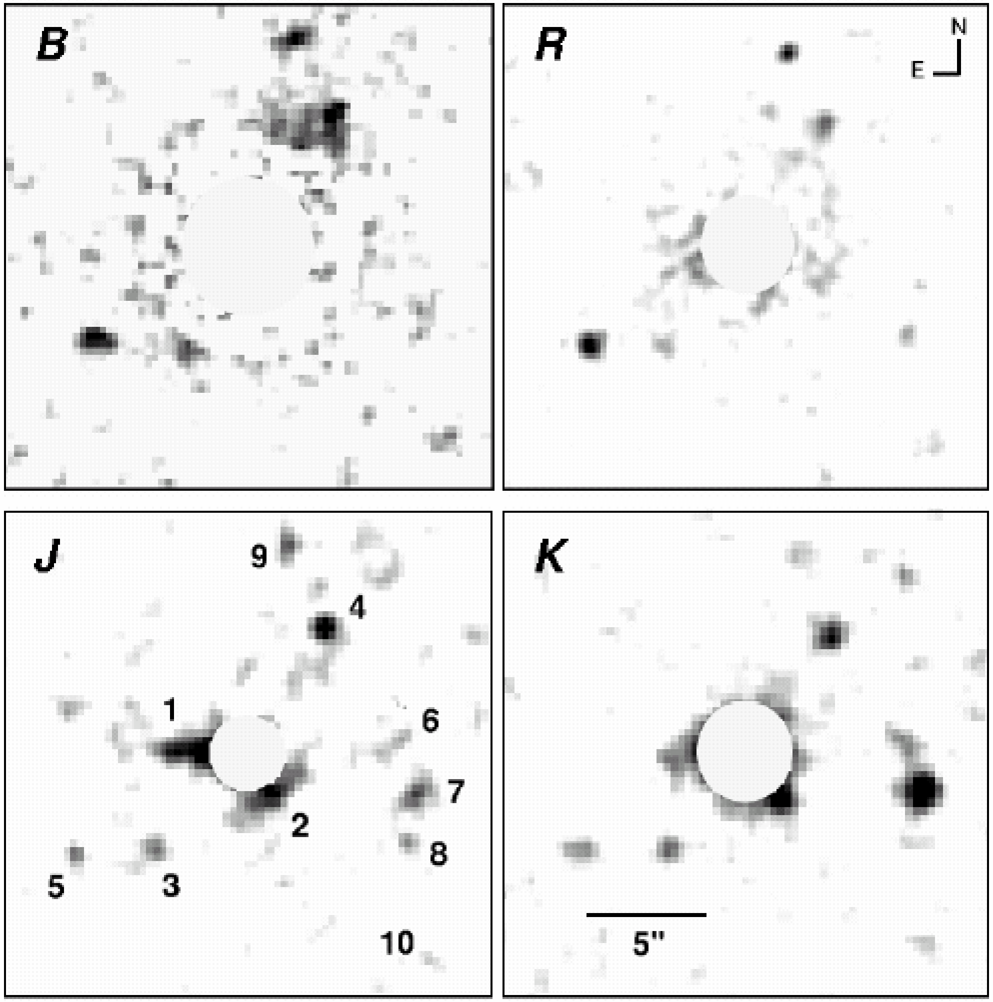

FIG. 3.—Smoothed B, R, J, and K images of the PKS 0952+179 field that contains a DLA system at $z = 0.239$. The PSF of the quasar has been subtracted in the B, R, and J images, but not in the K image, as there was no suitable PSF star in the field. The residuals in B, R, and J and the quasar in K have been masked. Objects are labeled only on the J image, for clarity. All 10 of these are detected in K. Features in the B and R images that lie at the edges of the mask are artifacts of the PSF subtraction process; only objects labeled 3, 4, 5, 8, 9, and 10 are detected in B, while those labeled 3, 4, 5, 7, 8, 9, and 10 are detected in R. Objects 1 and 2 are the best candidates for the DLA galaxy. Object 7 is an ERO, with $R-K = 6.5$. See § 3.2 for more details.

(Rao et al. 2003, ApJ, 595, 94)

Next, we add a new selection effect of DLA galaxies

(2) ***Masking effect***: fail to identify DLA galaxies hidden or contaminated by a point spread function of background QSOs

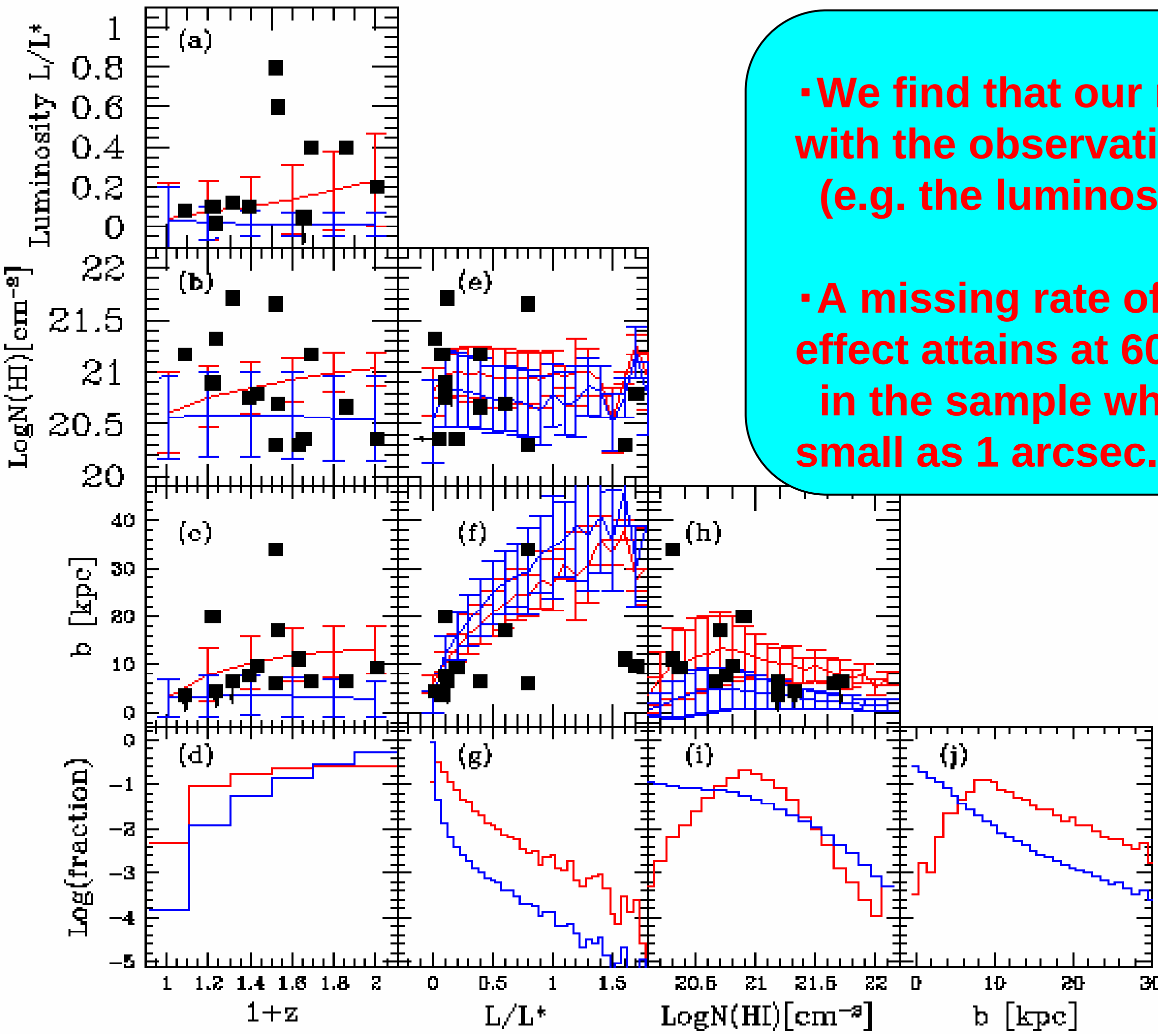

・We find that our results show better agreement with the observations (e.g. the luminosities and the sizes) .

・A missing rate of DLA galaxies by the masking effect attains at 60-80% in the sample when a angular size limit is as small as 1 arcsec.

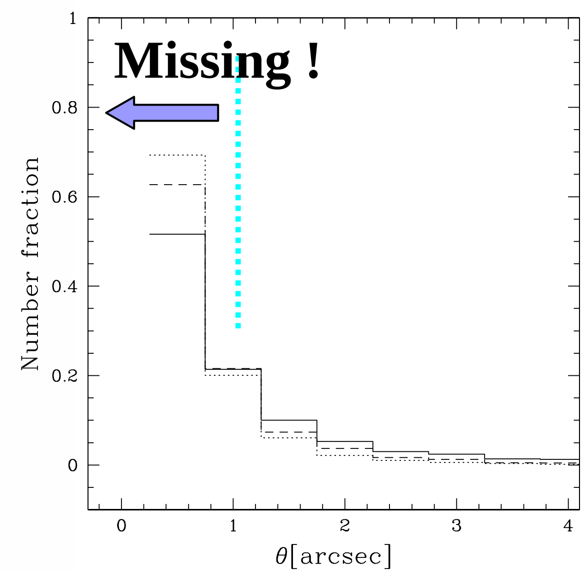

Radio Surveys

Another way to explore DLAs APART FROM THE SELECTION EFFECTS

- ***Arecibo Dual-Beam Survey (ADBS) [US]***

  Blind search for HI 21 cm emission covering ~430 deg^2 of sky

  The radio samples are 250-300 HI-selected galaxies

  (a) Detections of optical counterparts (Rosenberg et al.2005)

  ⟺ the 2MASS J-,H-,K-band observations ⇒ *L(J)-M(HI) relation??*

  (b) High N(HI) samples (Rosenberg & Schneider 2003)

  ⟺ Implication for DLA systems ⇒ *σ-M(HI) relation*

- ***HI Parkes All Sky Survey (HIPASS) [Australia]***

  Blind search the whole southern sky for HI 21cm emission

  (a) Extragalactic radio objects (Zwaan et al. 2003, 2005)

  ~4300 extragalactic HI objects

  (about 80% optical counterparts are confirmed: Doyle et al.2005)

  ⇒ HI Mass Function, Ω(HI), Dark galaxies..

  (b) Halo clouds (HVC) (Putman et al. 2003)

  ⇒ Missing satellites of the Local Group

  ⇒ CIV, MgII system

Blind HI surveys

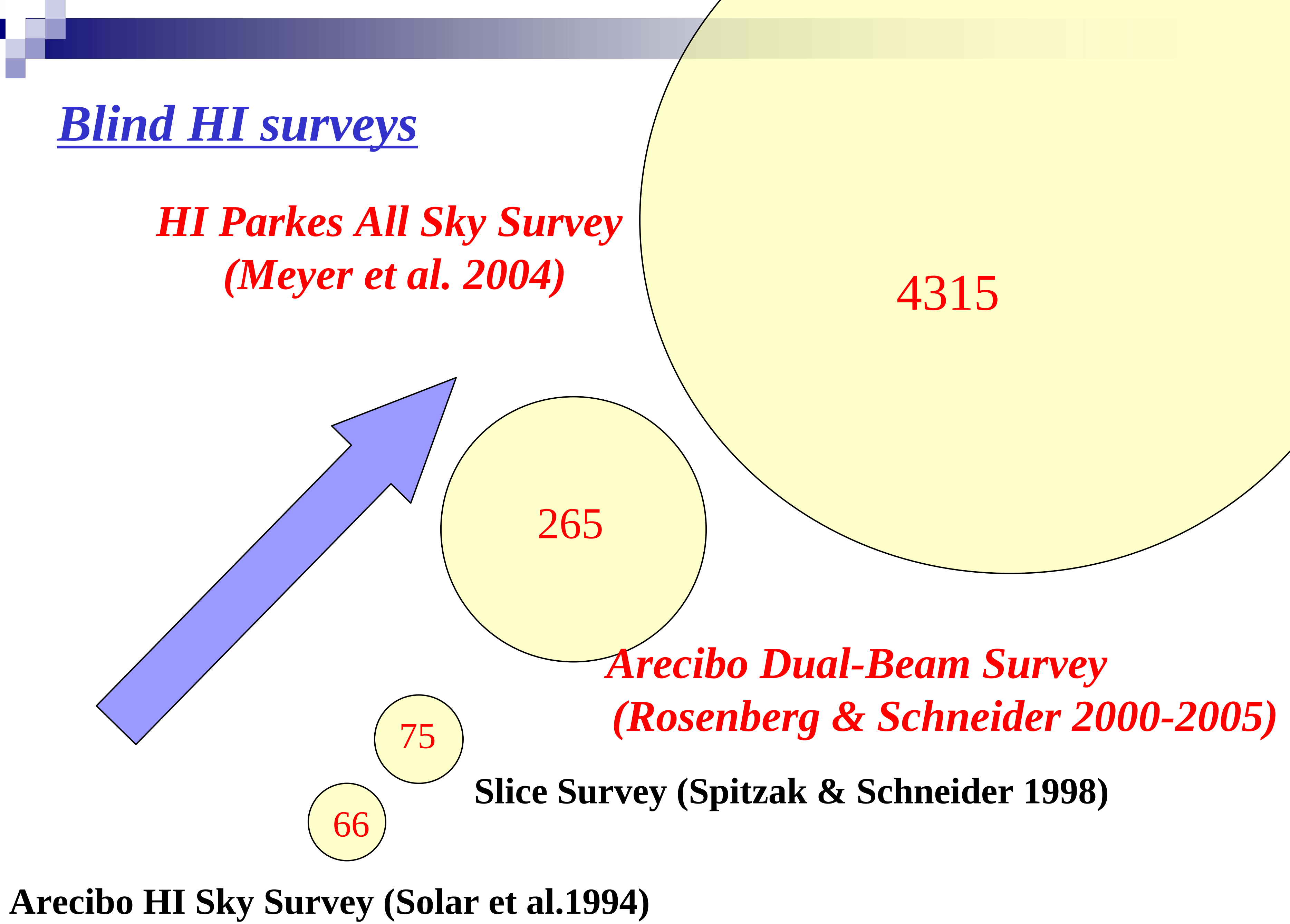

Disk Size vs HI mass

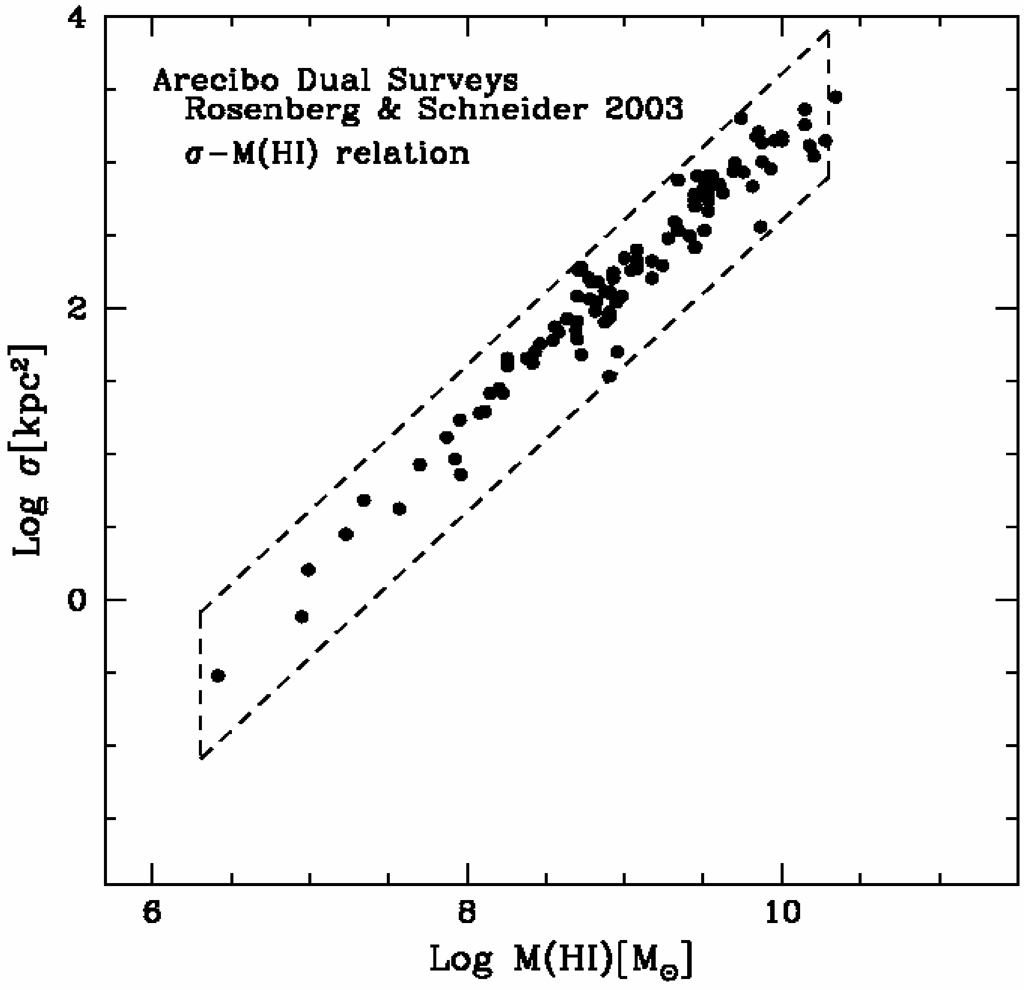

We find a tight correlation between the HI masses and the cross sections:
$\sigma \propto M(HI)^p$; p=0.97 ± 0.01

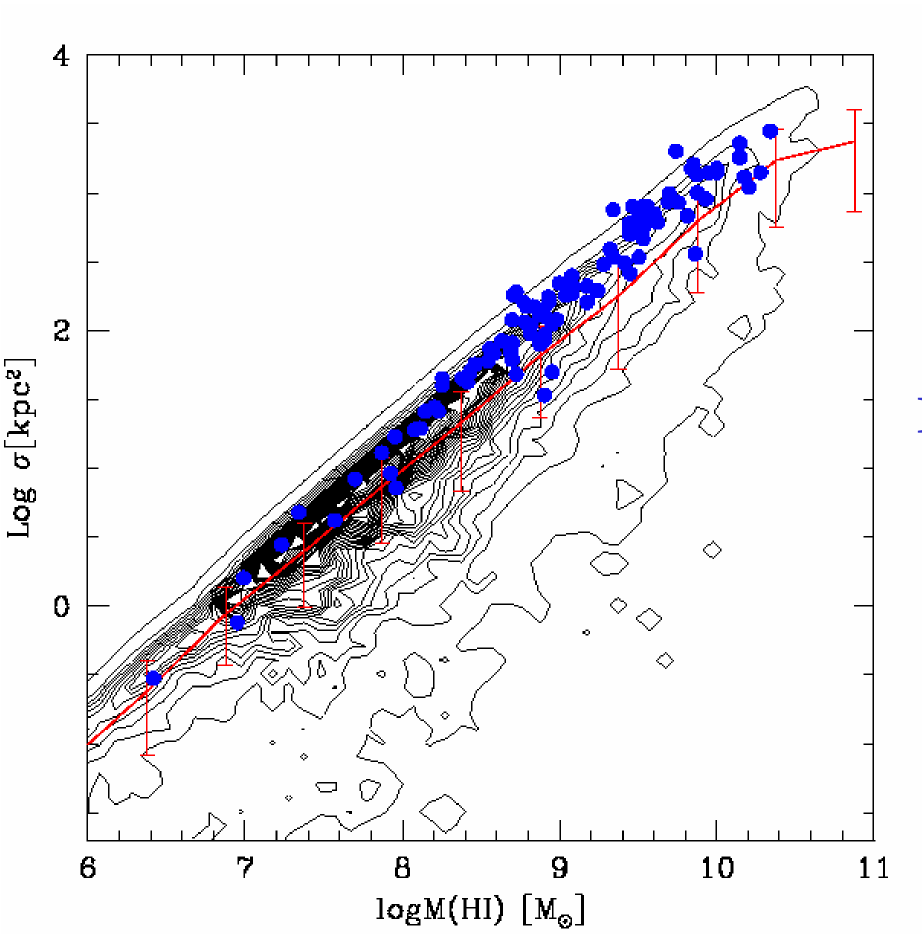

HI gas の拡がり, HI mass

Luminosty
(Star Formation) ?

DLA systems と galaxies との違いはあるのか？

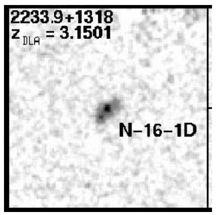

Luminosity

DLA systems
(QSO Absorption lines)

Galaxies
(Emission lines)

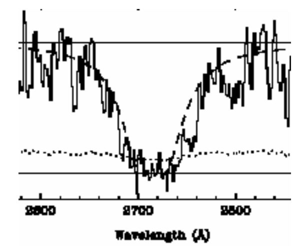

HI gas density

Optical Surveys
2MASS, SDSS, 2dFGRS,..
⇒ Emission lines(Hα,Lyα)
⇒ Stellar Mass
(Luminosity Function)

Blind Radio Surveys
HIPASS, ADBS,…
⇒ Emission lines(21cm)
⇒ HI Mass
(HI Mass Function)

Luminosity vs M(HI) relation

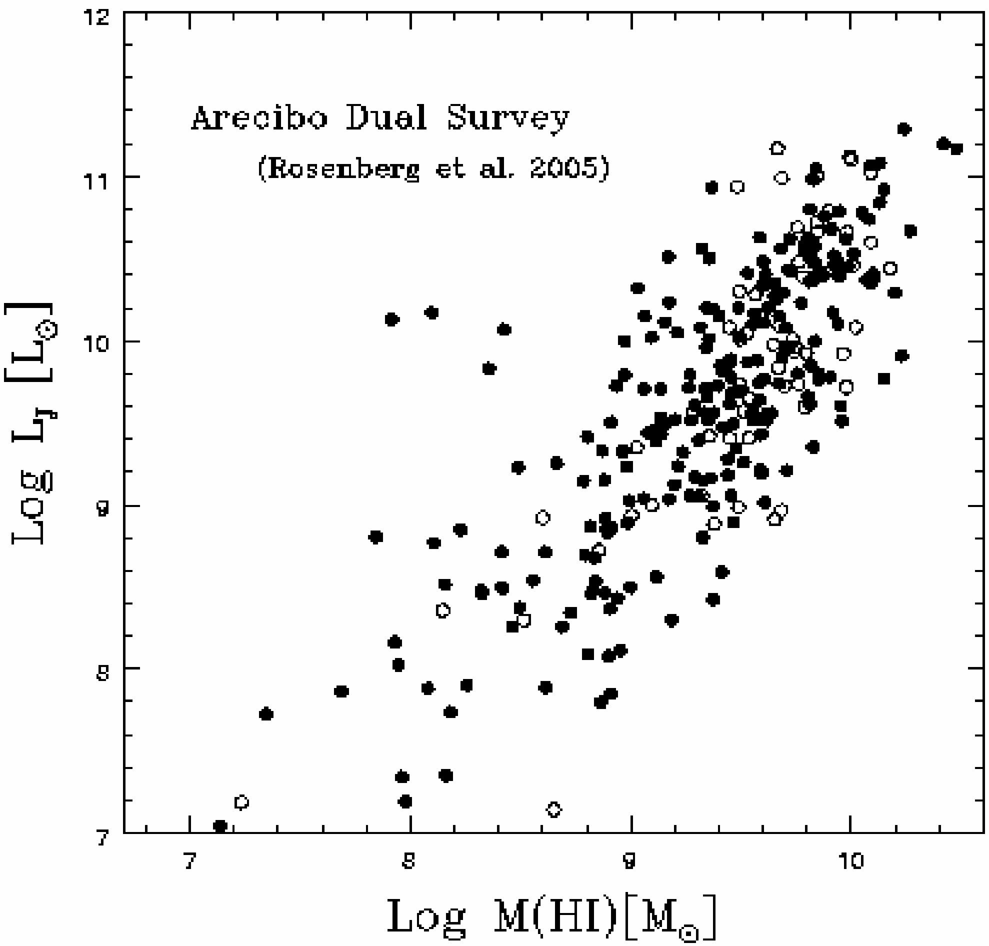

Our result agrees with the L(J)-M(HI) relation

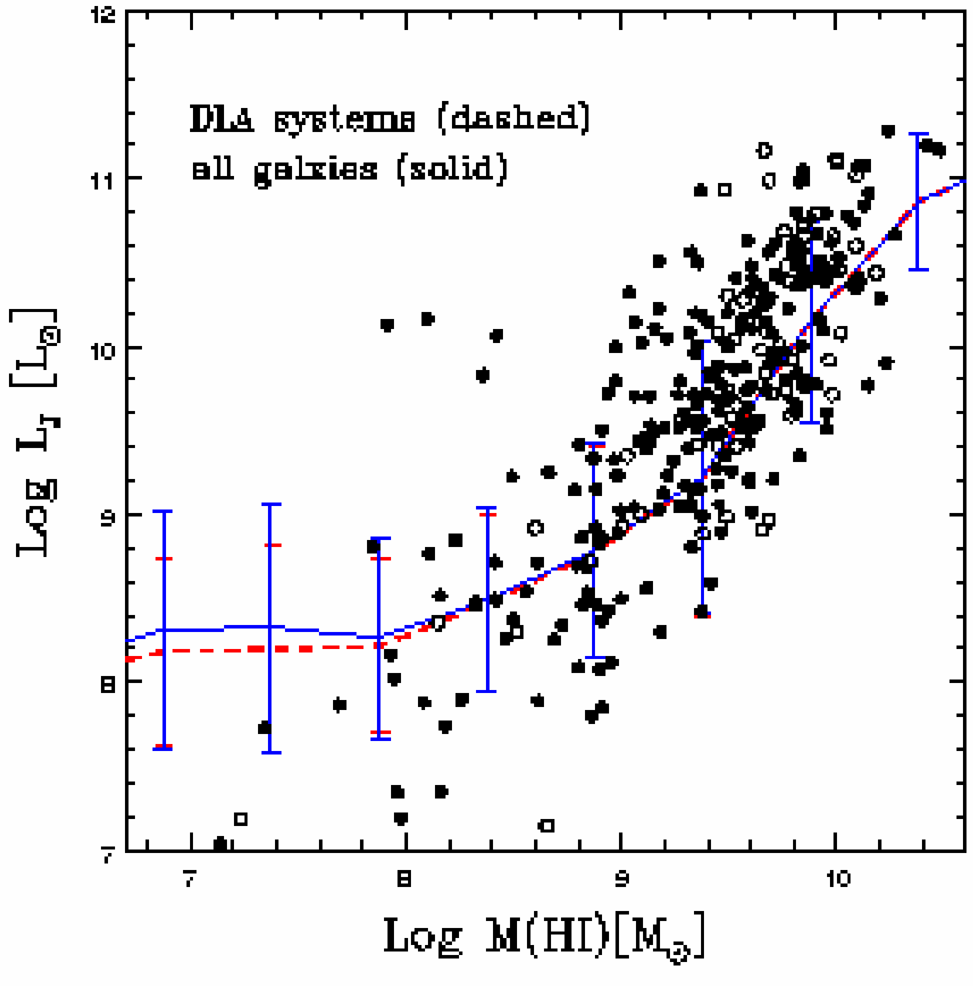

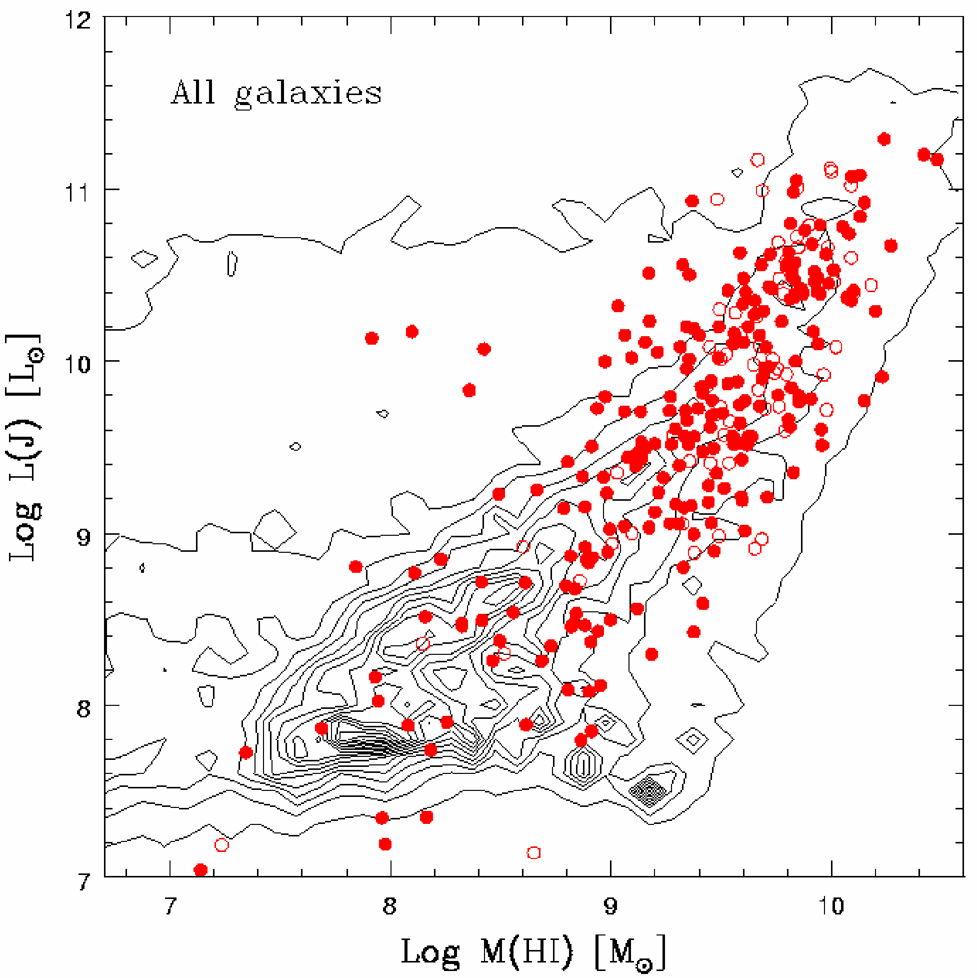
All galaxies
Log L(J) [L$_\odot$]
Log M(HI) [M$_\odot$]
12
11
10
9
8
7
7
8
9
10

No significant difference between DLAs and All galaxies!

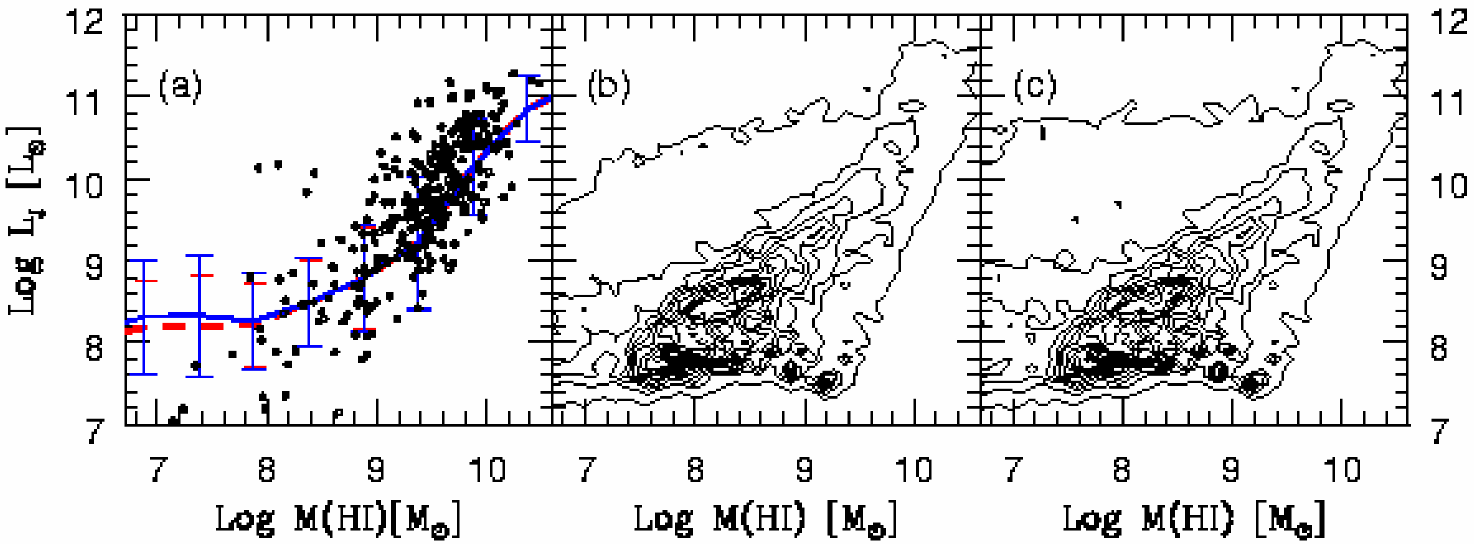

HI Mass Function (HIMF)

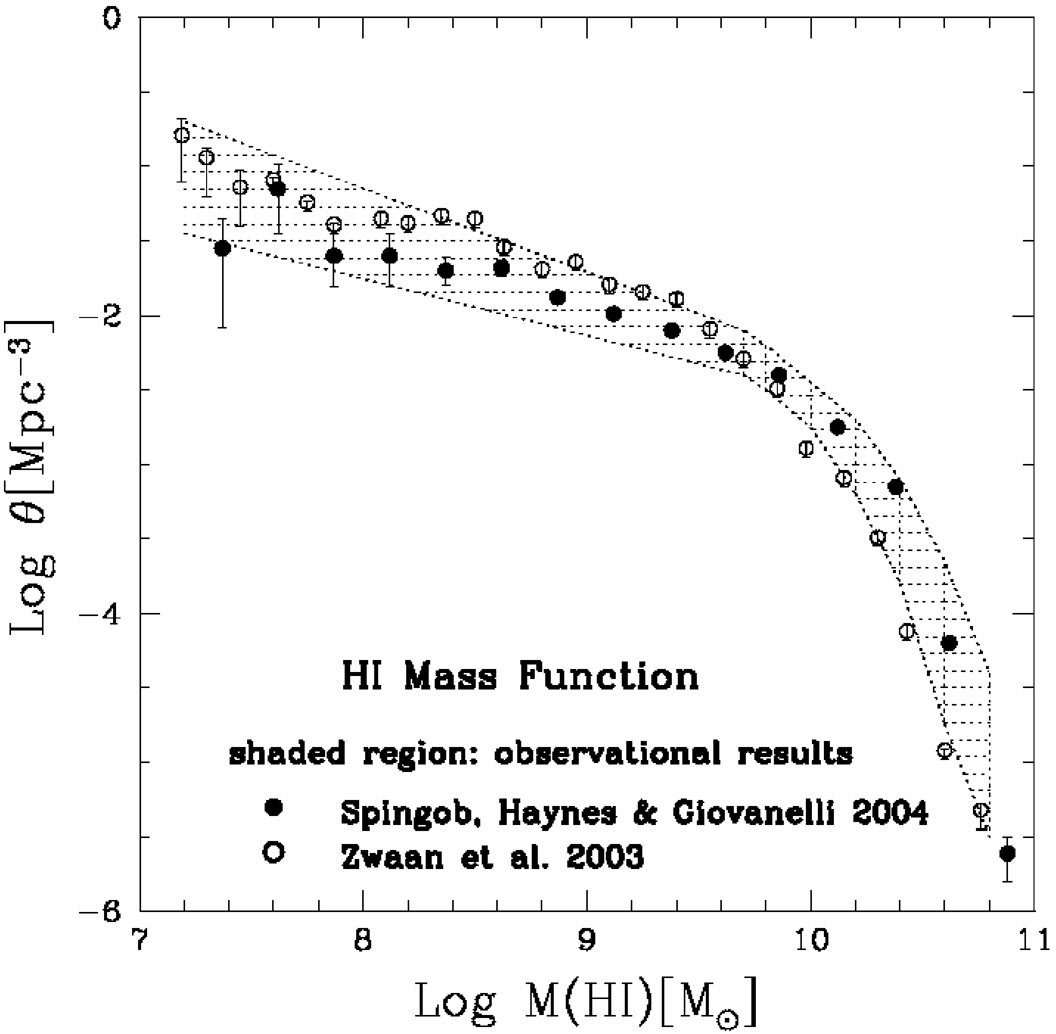

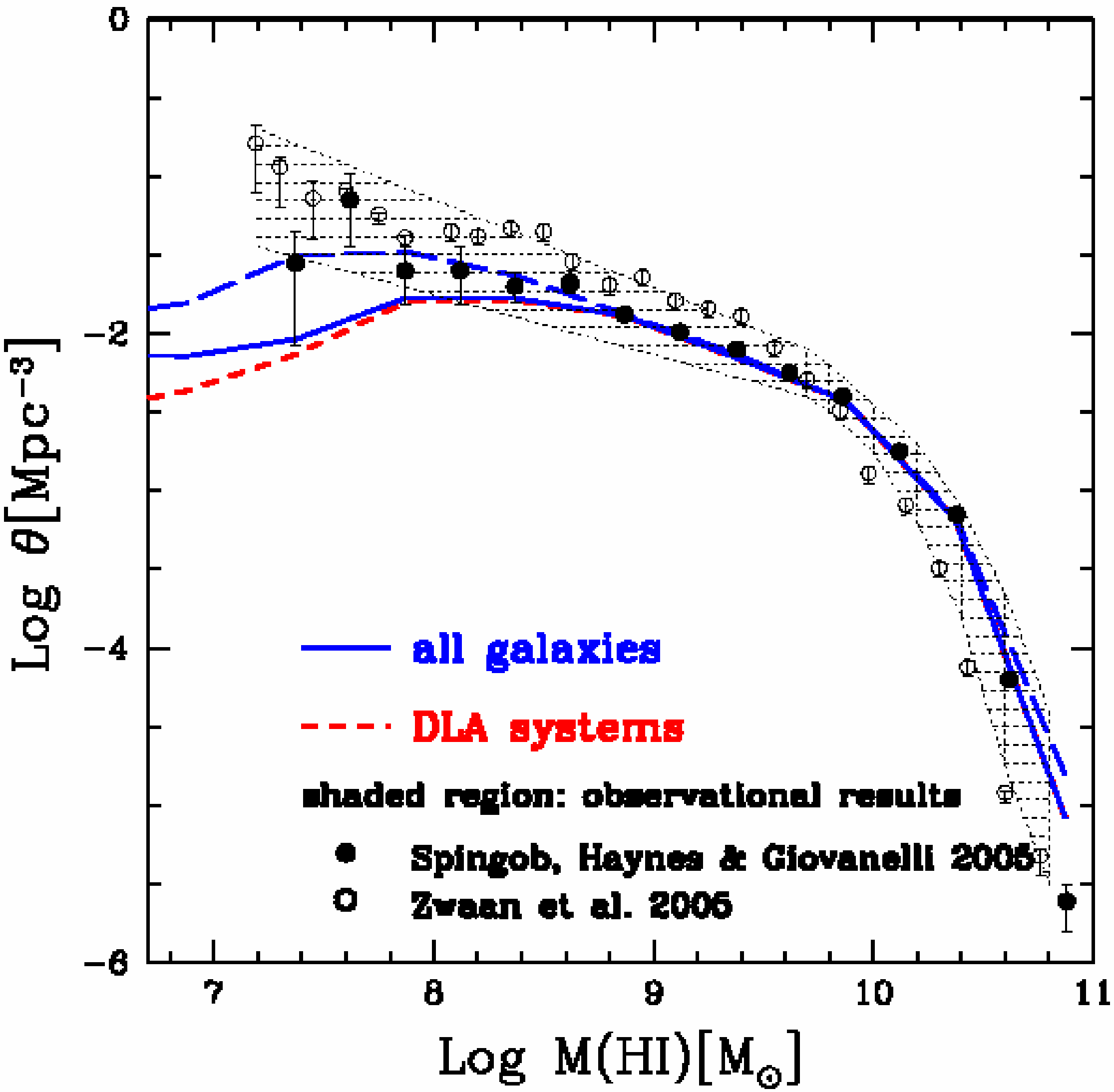

Our results are consistent with the observations at $M>10^8 M_\odot$

DLA systems

⇒ HI-Selected galaxies at $M>10^8 M_\odot$

Prediction: SFR -M(HI) relation

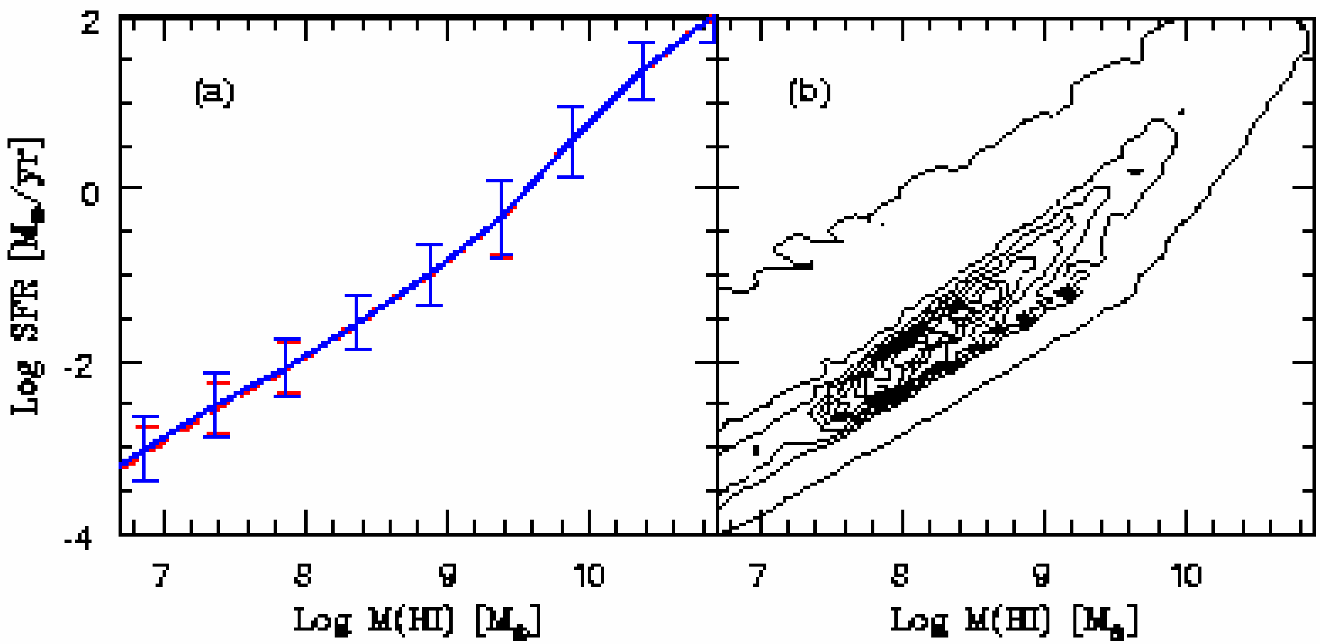

The SFR is correlated more tightly with the HI mass

$SFR \propto M(HI)^{\alpha}$ α=1.22±0.05

Recent Observational Results

- Optical Surveys for HI-selected Galaxies

  SINGG (Survey for Ionization in Neutral-Gas Galaxies)

  H-alpha emission lines from HIPASS galaxies

  (e.g. Meurer et al. 2006 ApJS, 165, 307)

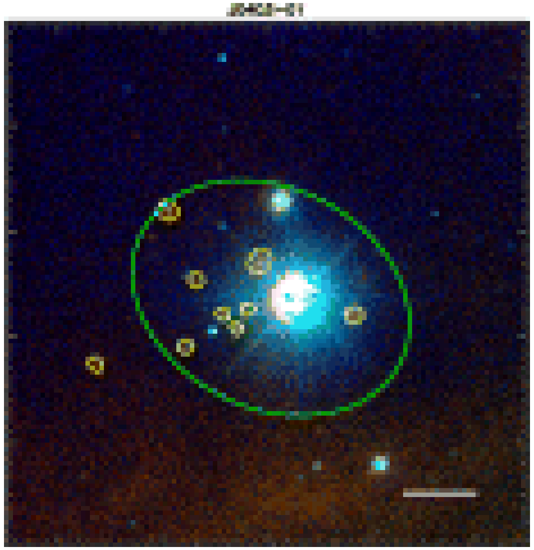

93 HIPASS targets ⇒ Star Formation Rates

HIPSS Catalogue: Optical Counterparts of HI Selected Galaxies (Doyle et al. 2005)

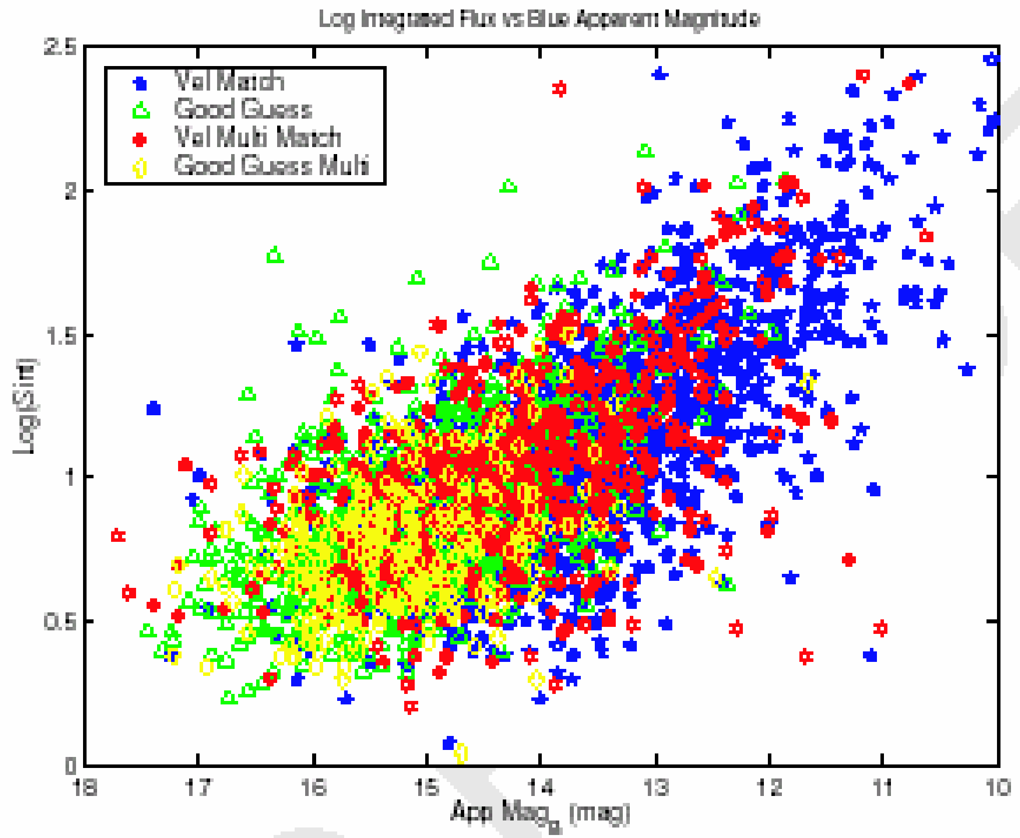

Figure 7. Log (integrated H I radio flux) versus B_J apparent magnitudes for the optically matched HICAT sources. Match categories are listed in the insert. This shows there is a clear trend that, the brighter the optical magnitude, the larger the H I radio flux.

Optical Counterparts of ADBS samples

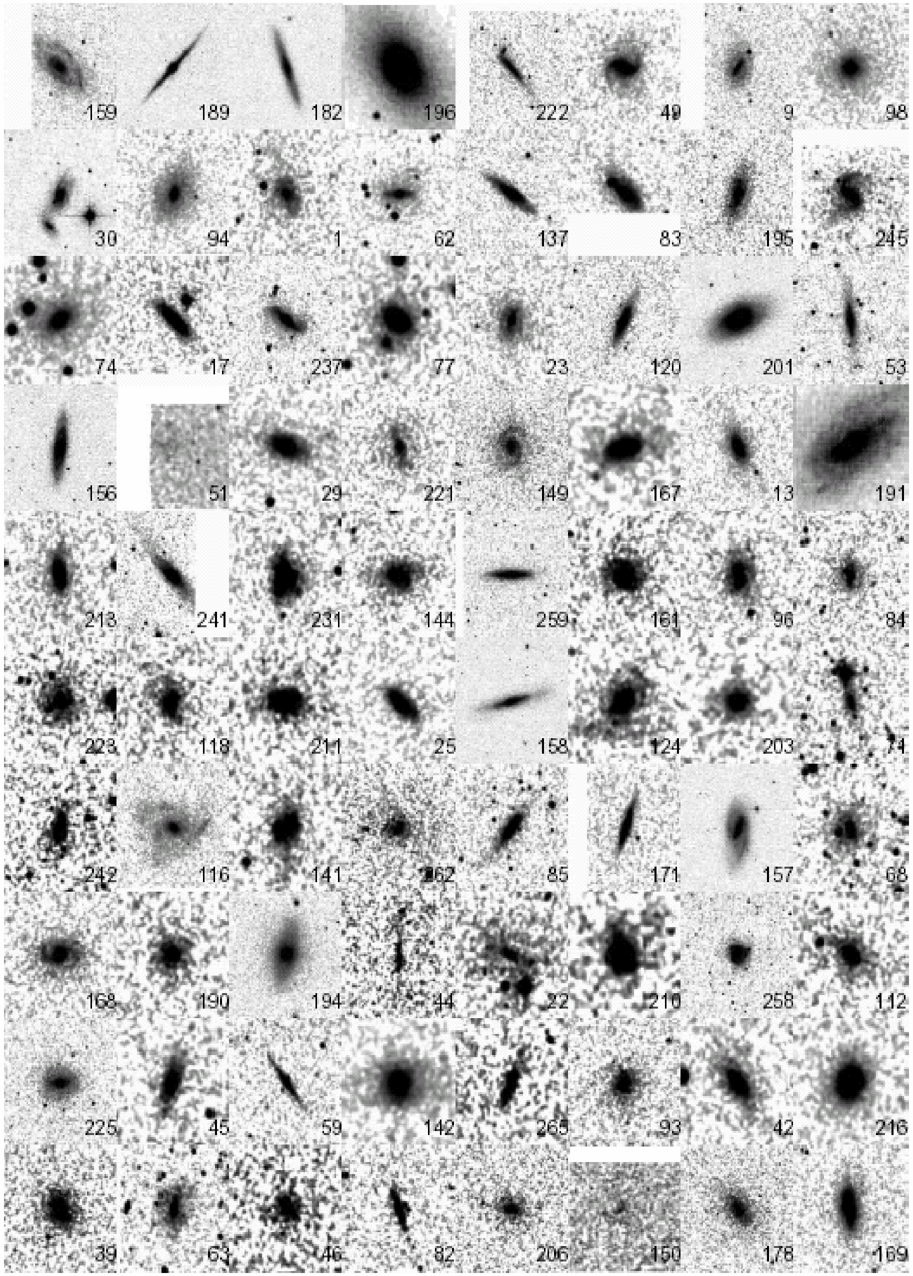

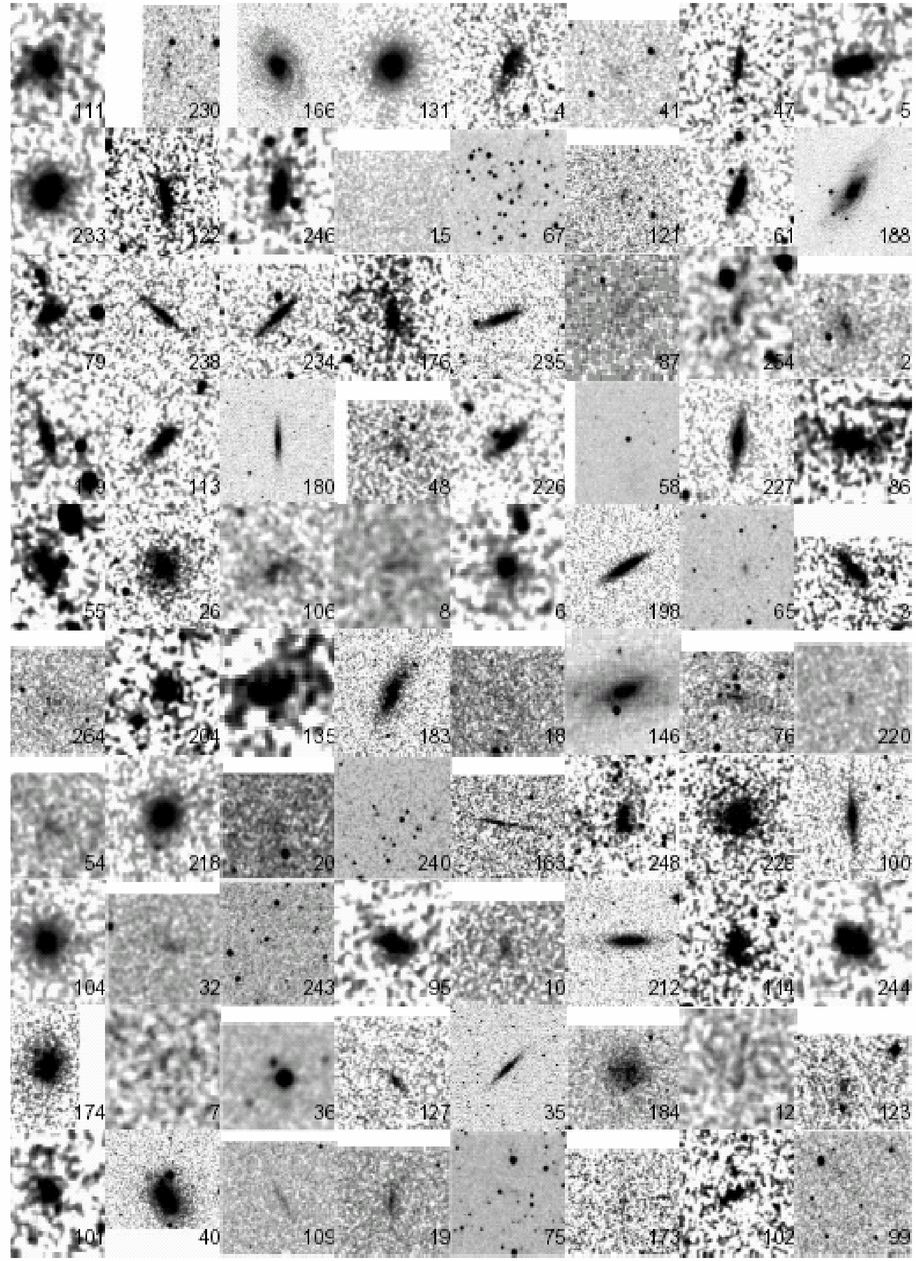

FIG. 10b

Good Agreement with the SFR-M(HI) Relation

- **More samples of low-M(HI) systems !**

  HI-selected galaxies provide good clues for determining the SFRs

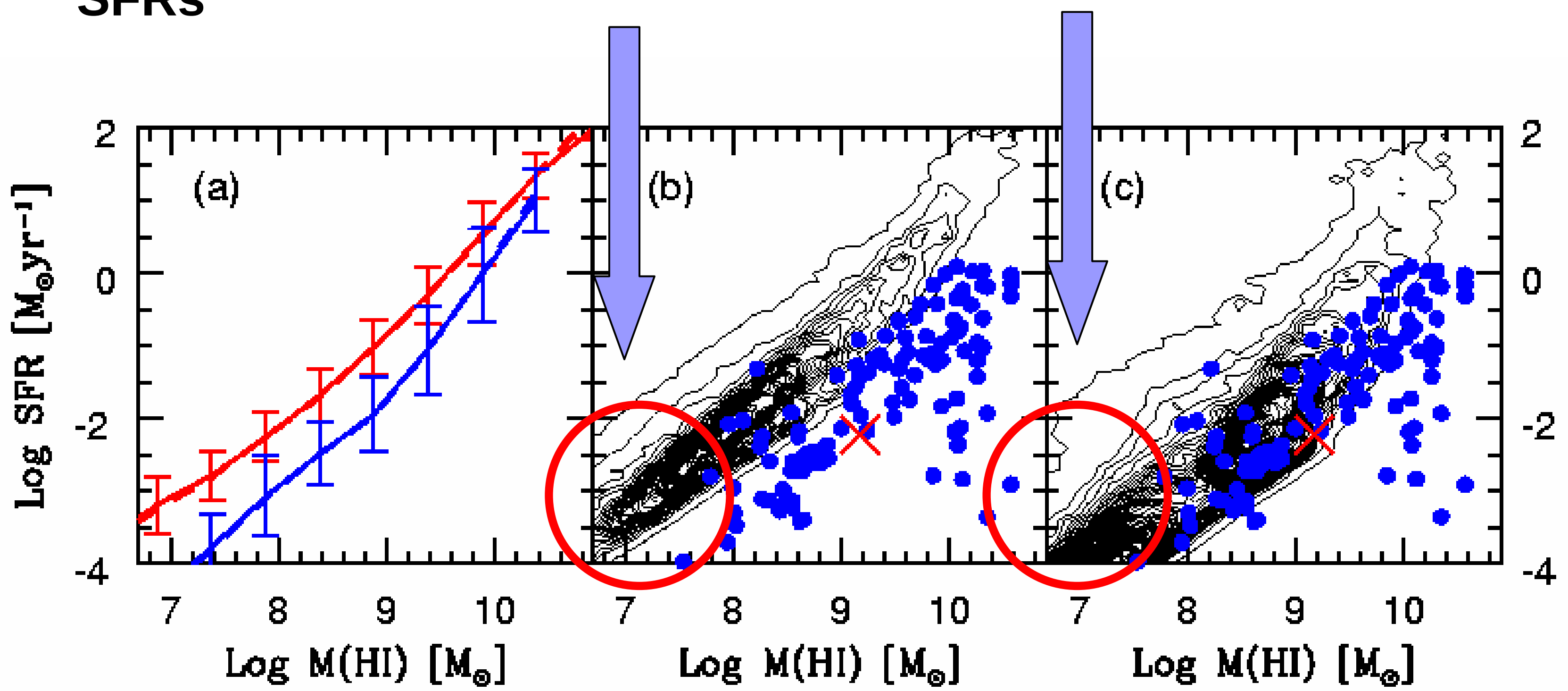

Our model suggests that the average SFRs 0.01 $M_\odot$ /yr.

[C] *Radio properties of DLA systems at redshift z=0*

Another way to explore DLA systems apart from selection effects.

Detection of DLA galaxies by Blind 21cm surveys (e.g. Rosenberg & Schneider 2003)

⇒ about 50 HI-rich galaxies with HI column densities comparable to those in DLA systems

We find that

(1) A tight correlation between the HI masses and the cross sections: Log $\sigma \propto$ Log M(HI)

(2) HI-rich galaxies with 10^9$M_\odot$ mainly contribute to the population of DLA systems at z=0

⇒ Our result is entirely consistent with the observational properties of HI-selected galaxies in the radio survey.

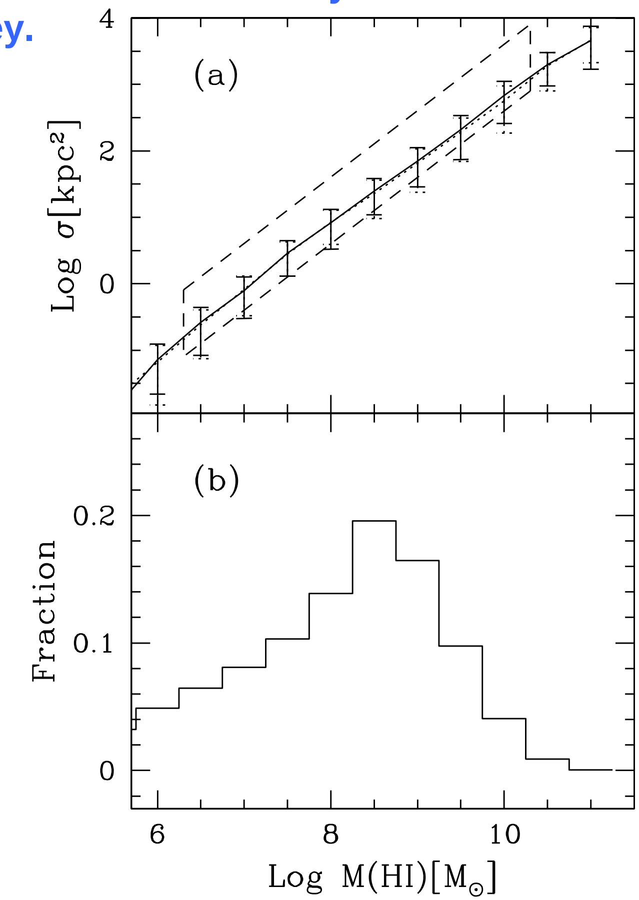

Dashed box: observational data (Rosenberg & Scheider 2003)

[D] Star formation rates (SFRs)

a clue to exploring what types of galaxies consist of DLAs

⇒ Our model suggests that the average SFRs are as low as 0.01 $M_\odot$ /yr.

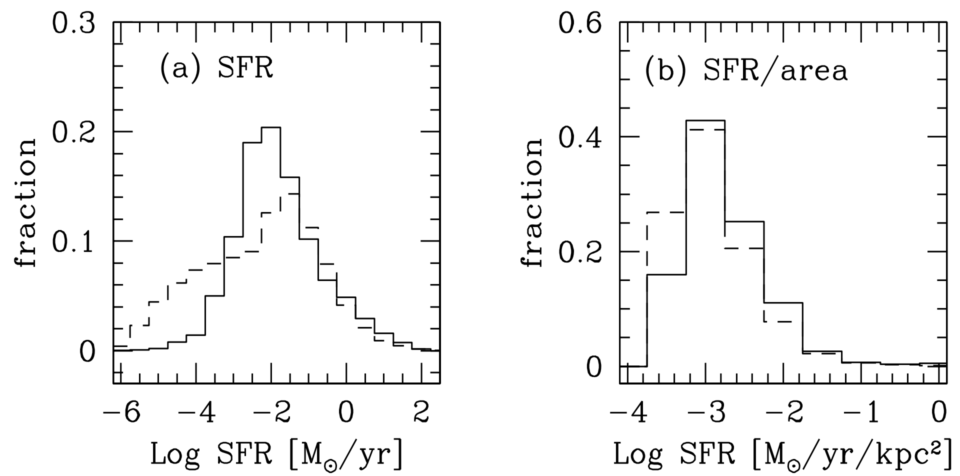

Conclusions

●We investigate evolution of Damped Lyman α systems taking into account merging processes of dark halos from hierarchical galaxy formation models

Our results are *simultaneously* consistent with the observational properties:

DLA systems: Metallicity evolution, N(HI)-distribution

Optically selected-galaxies:
Luminosity functions, HI-gas mass fraction

Radio selected-galaxies:
HI-disk size, Luminosities(J-band), HIMF, Ω(HI)

LSB dwarf galaxies primarily contribute to the population of DLA systems at z<1: size ~3kpc, Sb ~22 to 27 mag arcsec^{-1},SFR ~10^{-2} $M_{\odot} yr^{-1}$

DLA corresponds to HI-selected galaxies at M(HI)>$10^8 M_{\odot}$ in blind Radio Surveys (ADBS, HIPASS)
(NB: sub-DLA corresponds to HIPASS galaxies at M(HI)~$10^7 M_{\odot}$) (Okoshi et al.2007)
⇒ Our prediction: more tight relation: SFR-M(HI) relation

High redshisft (z>2) vs Low redshift (z<2)

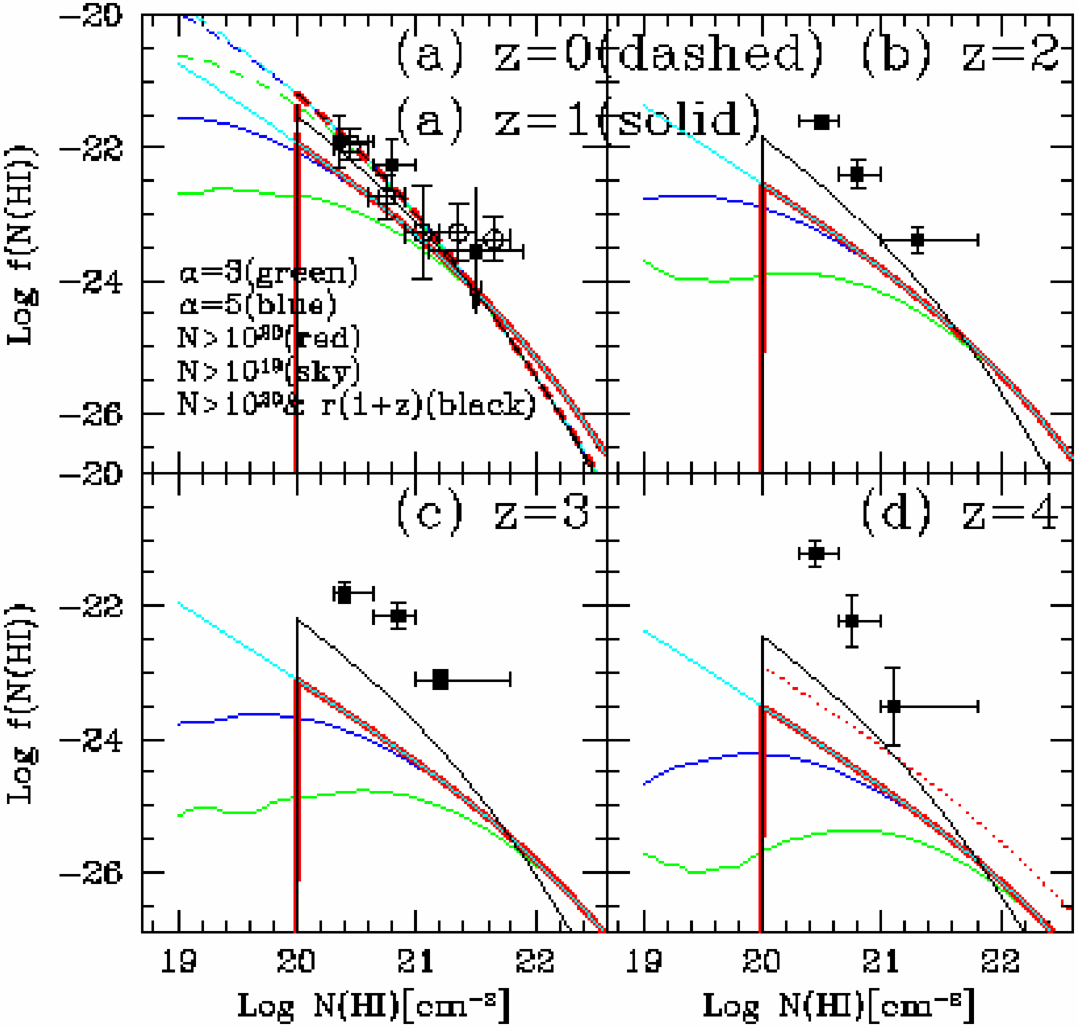

Different Population??

$$\frac{dN}{dz} = n\pi r^2 \frac{c}{H(z)}(1+z)^2$$

$$= 0.20 \left(\frac{r}{19\ h^{-1}\ \mathrm{kpc}}\right)^2 \frac{n}{0.016\ h^3\ \mathrm{Mpc}^{-3}}$$

Number density
vs
Cross section

Difficulties for realizing high-z DLA disks

How one can form rotaionally supported disks ~ 20 h^{-1}kpc at z>2 ?

Tidal torques provide 5-10 % of the angular momentum for rotational support

The radius of gas sphere at turn-around **is ~200 h^{-1}kpc**

Spherical top-hat flactuation ⇒ collapse timescale

$$t_{coll} \sim 2t_{dyn} \sim \pi \left(\frac{2GM}{R^3}\right)^{-1/2} \sim 3Gyr \left(\frac{M}{10^{12}M_\odot}\right)^{-1/2} \left(\frac{r_m}{200\mathrm{kpc}}\right)^{3/2}$$

Need for some information about
Spatial distribution : tidal tail, caustics or panckaes

Theoretical Models [準解析的手法とNumerical Simulations]

- *Nagamine, Springel, Hernquist (SPH)*
  DLAs ⇒ Compact objects $M_{DLA}=10^{11.2}M_{\odot}$

  Too high metallicity ⇒ Strong Wind Model (Low resolution?)

- *Bouche, Gardner, Katz, Hernquist, Weinberg*
  DLAs ⇒ (massive) galaxies with large disks

  Halo mass $M\sim10^{10}\ M_{\odot}$以下のハローに対して、cross-section vs circular velocityの関係（$\sigma\propto Vc^{\beta}$）を外挿して考察

  Too large cross-sections (Low resolution?)

- *Maller, Somerville, Primack (SAM)*
  DLAs ⇒ galaxies with Mestel-type disks $N(HI)\propto R^{-1}$

  α_*は考慮されていないため、**metallicity evolutionは再現できず。**
  dN/dN(HI)やLarge cross-sectionも説明できず。

Results of Numerical Simulations

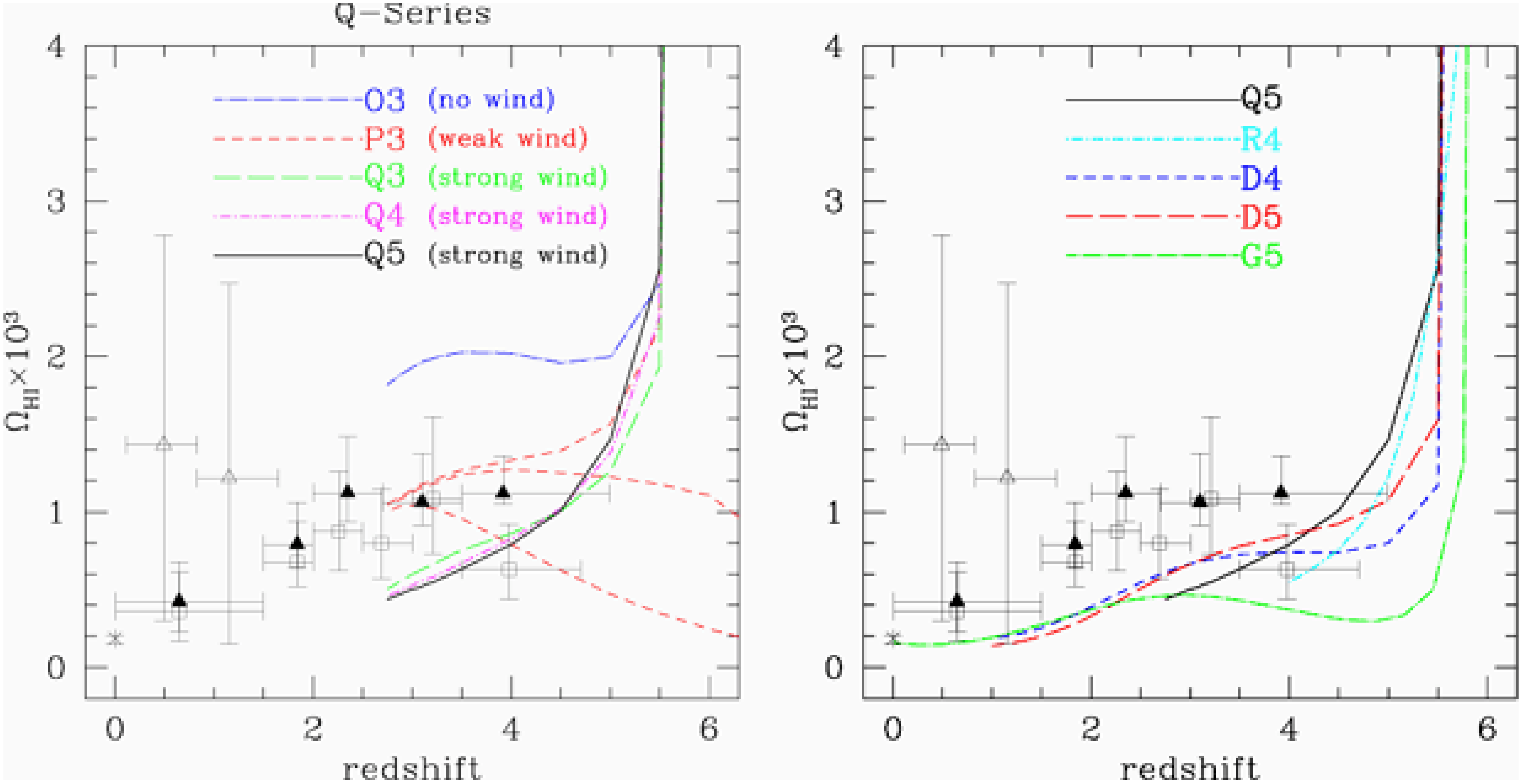

SPH: Nagamine et al. 2004

これまでの結果

- **DLAs correspond to HI-selected galaxies at $M(HI)>10^8 M_\odot$ in blind Radio Surveys (ADBS, HIPASS)**
  ⇒ ***Our prediction: more tight relation: SFR-M(HI) relation***

- **DLAs are LSB dwarf galaxies (~3kpc) at z<1**

Our results are entirely consistent with the observational results of the counterparts:

(a) DLAs [HST]: Lanzetta et al.2002
Rao et al. 2003, Hopkins et al.2005
(b) HI selected galaxies [BRS]: Rosenberg et al. 2005

COMPACT OBJECTS

High redshift z では？

Detection of Lyman alpha emission from DLA-host galaxies

Moller, Fynbo & Fall 2004, A&A 422,L33

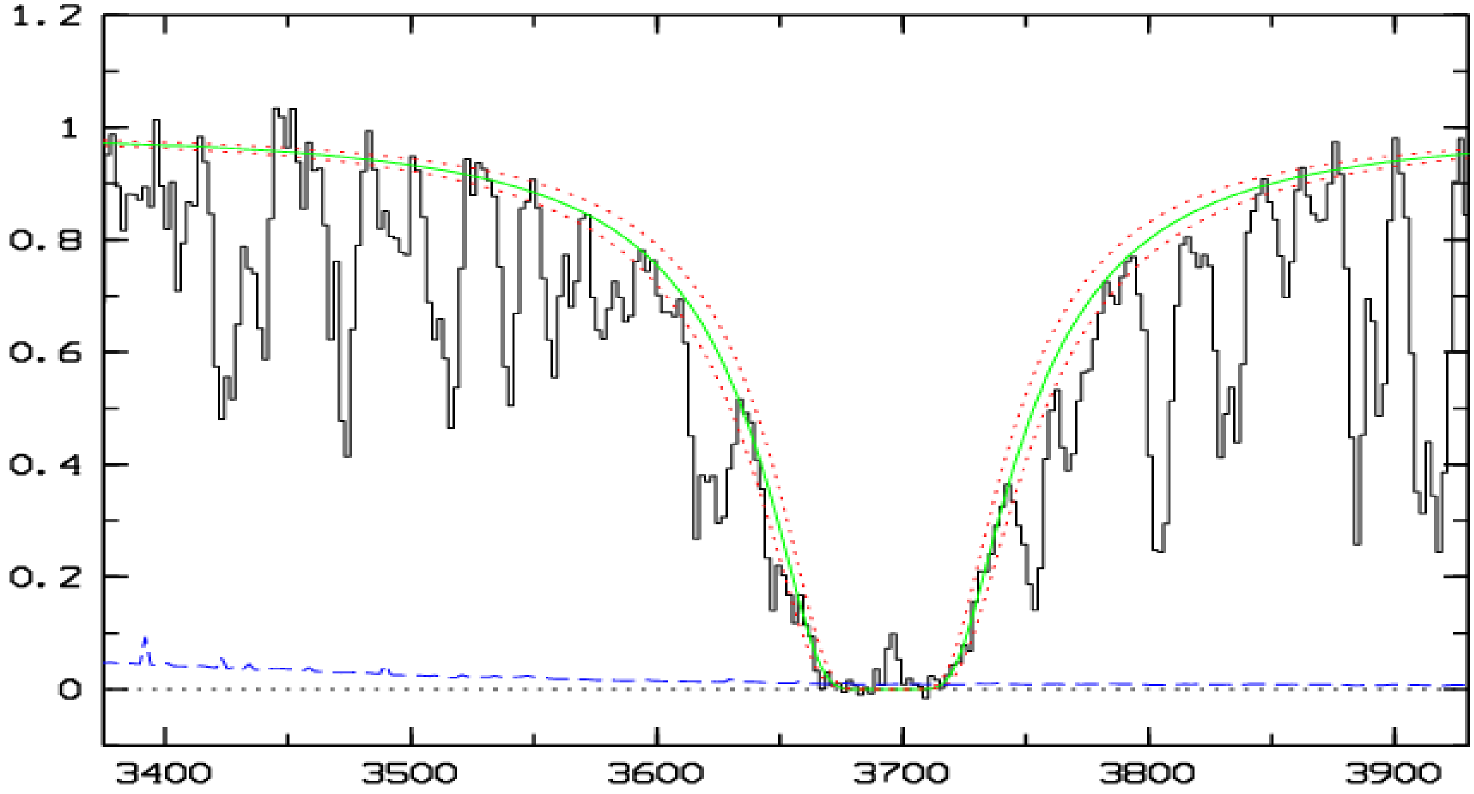

FORS1/G600B spectrum of the z=2.0395 Damped Ly line. The 1 noise spectrum (per 5 Å resolution element) is shown as a dashed line (blue). The emission line is detected at 9.3 sigma .

2D spectra of a DLA at z=2.0395

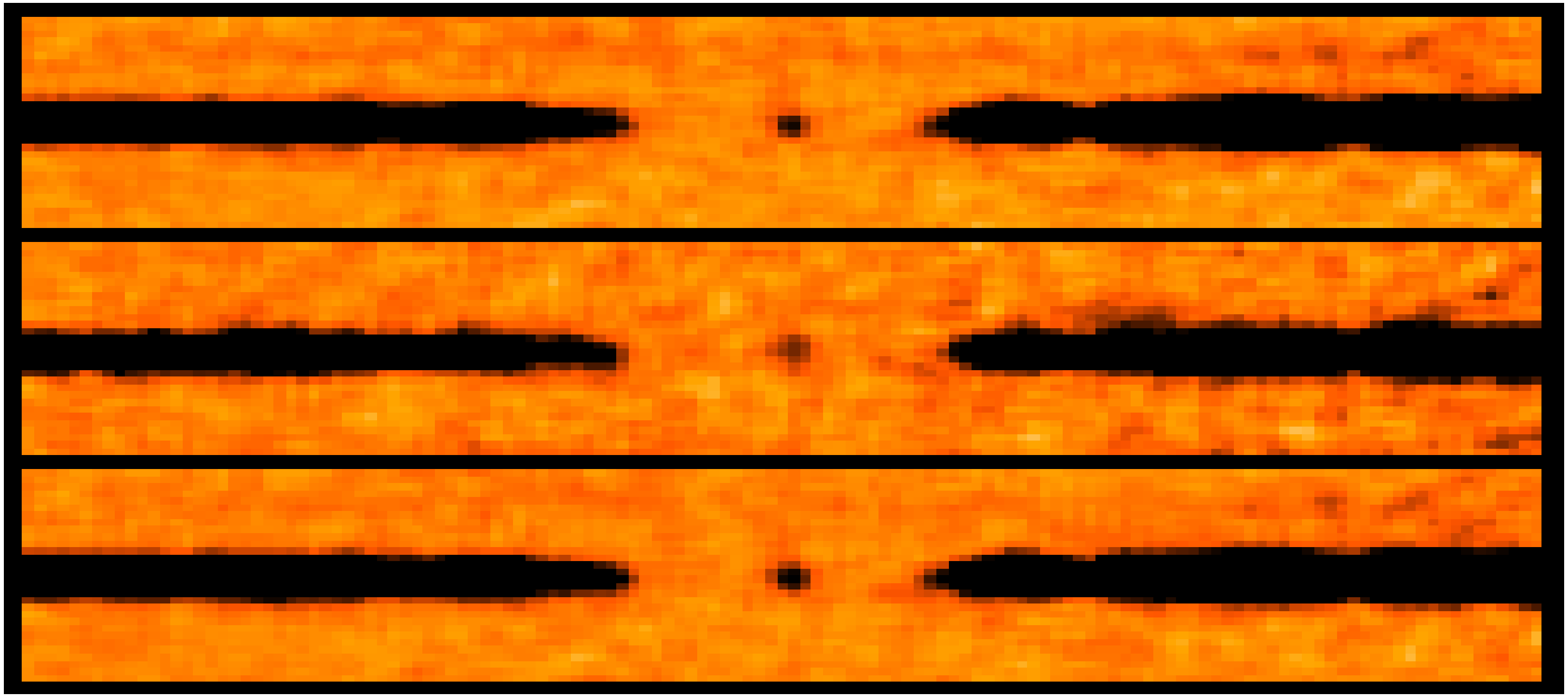

DLA galaxies at high redshift detected in emission

Table 2. Lyα emission and metallicity data for five $z \geq 1.9$ DLA galaxies. b_{DLA} is the impact parameter, log (N) is the HI column density, and Δv is the difference between DLA redshift and QSO redshift given in km s^{-1}. The "Type" classifications in the last column are defined as "$z_a \approx z_e$": $|\Delta v| \leq 3000$ km s^{-1}; "sub-DLA": log (N) ≤ 20.3; "DLA": classic intervening non-sub DLAs.

ID	NICMOS ID	z_{DLA}	b_{DLA} "	Emission refs.	log (N) cm^{-2}	[M/H]	M	[M/H] refs.	z_{QSO}	Δv km s^{-1}	Type
DLAg0528–25	N-7-1C	2.8110	1.14(2)	1, 3, 5, 10, 11	21.35	–0.75, –0.76	Si, Zn	14, 15	2.797	–1100	$z_a \approx z_e$
sDLAg2233+13	N-16-1D	3.1493	2.51(2)	2, 4, 10, 11, 12	20.00	≥–1.04	Si	16	3.298	10 500	sub-DLA
DLAg0151+04	–	1.9342	0.93	6, 7, 8, 9	20.36				1.922	–1200	$z_a \approx z_e$
DLAg2206–19	N-14-1C	1.9205	0.99(2)	10, 11	20.65	–0.39, –0.42	Zn, Si	15, 17	2.559	58 600	DLA
DLAg0458–02	–	2.0396	0.3(3)	13	21.78	–1.17, –1.19	Zn, Zn	15, 17	2.286	23 300	DLA

(1) Møller & Warren (1993); (2) Steidel et al. (1995); (3) Warren & Møller (1996); (4) Djorgovski et al. (1996); (5) Møller & Warren (1998); (6) Møller et al. (1998); (7) Fynbo et al. (1999); (8) Møller (1999); (9) Fynbo et al. (2000); (10) Warren et al. (2001); (11) Møller et al. (2002); (12) Christensen et al. (2004); (13) this paper; (14) Lu et al. (1996); (15) Kulkarni & Fall (2002); (16) Lu et al. (1998); (17) Prochaska et al. (2003).

High-z DLA galaxies are also very COMAPCT !?

⇒MORE samples are required to study high-z DLA galaxies

⇒ The difficulties of detecting the emission lines;

Compactness, Low Surface Brightness,…

Half-light radius & Optical to NIR color of high-z DLA galaxies

(Moller et al. 2002, ApJ, 574,51)

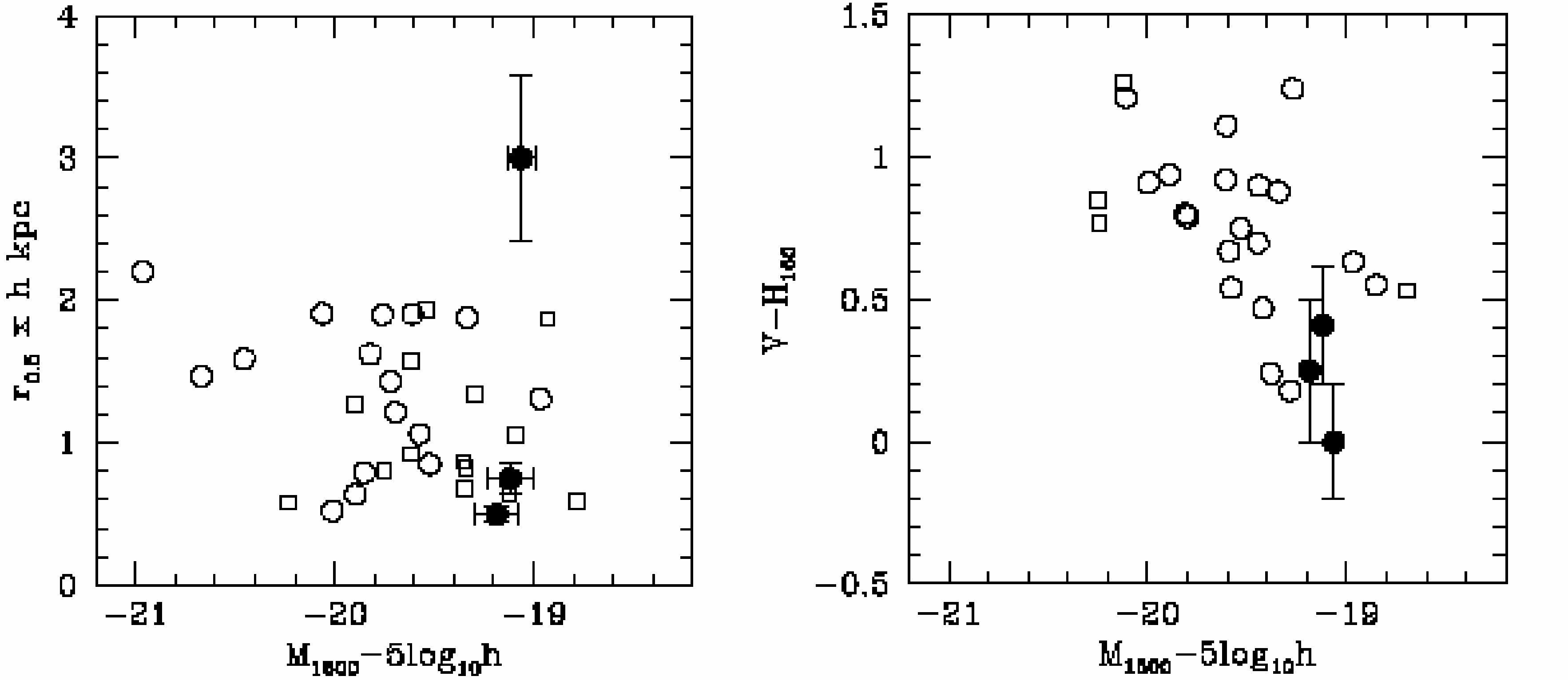

FIG. 3.—*Left*: Half-light radius vs. absolute magnitude for 21 HDF-N LBGs with $2.0 < z < 3.5$, measured by Marleau & Simard (1998), and the three DLA galaxies. The 16 LBGs consisting of a single component are plotted as open circles. The 14 components of the remaining five LBGs are plotted as open squares. The three DLA galaxies are plotted as filled circles. The DLA galaxies have half-light radii in the same range as the LBGs of similar absolute magnitude. *Right*: Optical to near-infrared $V-H_{160}$ color vs. absolute magnitude for the same 21 LBGs and three DLA galaxies, using the same symbols. The colors of the LBGs are taken from Papovich et al. (2001). Their catalog differs from that of Marleau & Simard (1998) in terms of the number of galaxy components, with 19 single galaxies plus two galaxies with a total of four components. Therefore, we have used the V_{606} magnitudes of Papovich et al. to calculate absolute magnitudes. The DLA galaxies have colors similar to those of the Lyman break galaxies of similar absolute magnitude.

Relation between DLAs and LBGs

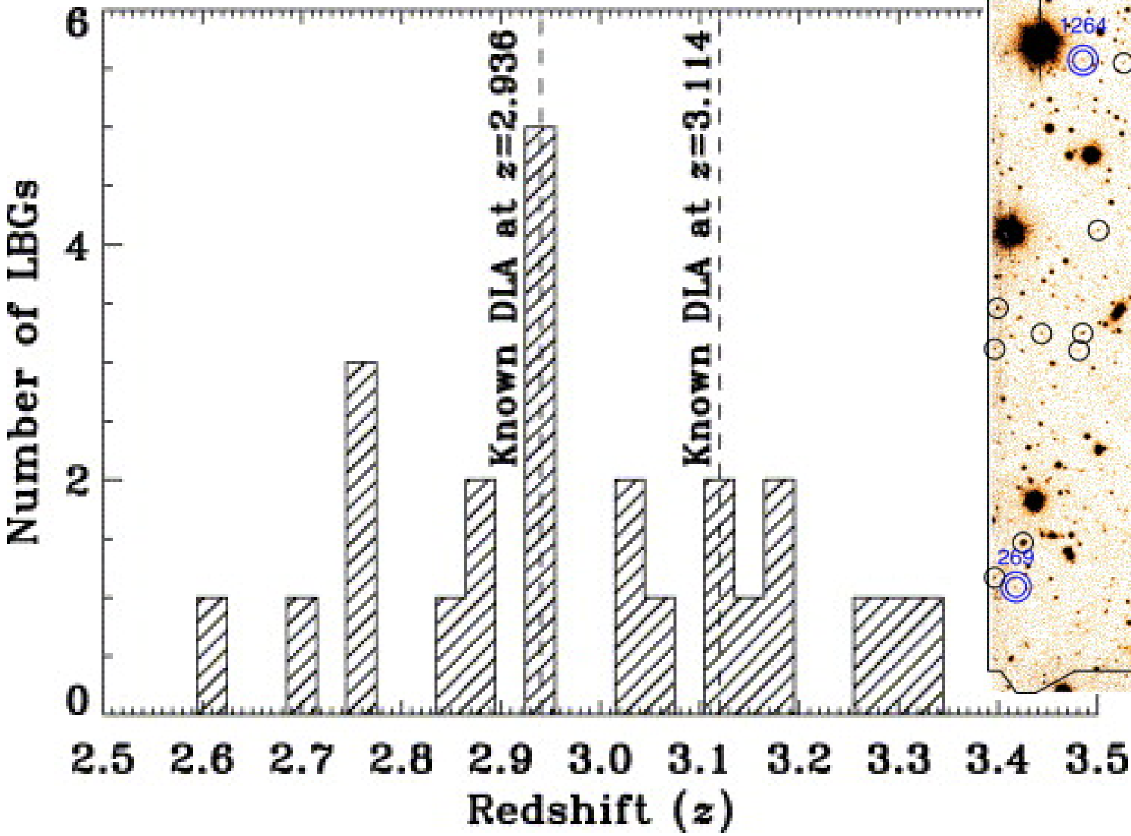

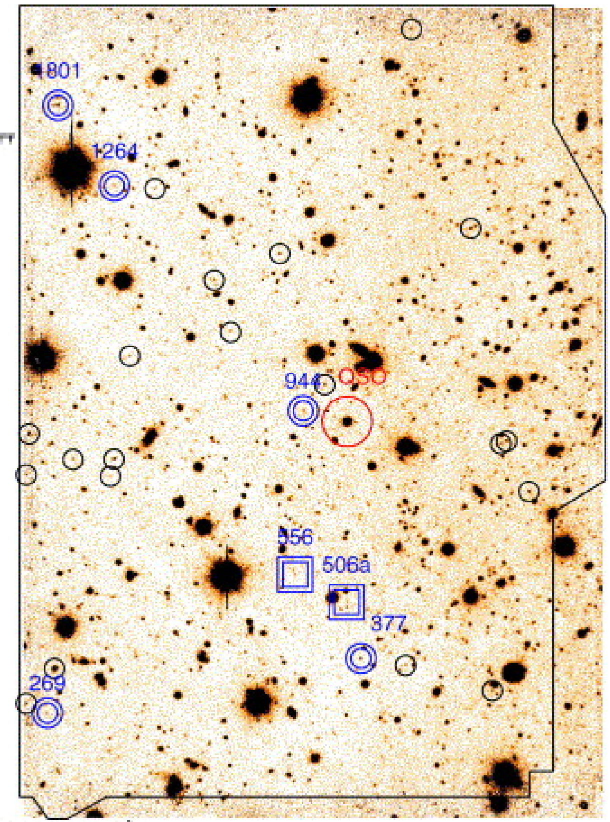

Fig. 1. PSS0808+5215 redshift histogram. Redshift histogram of the $2.6 < z < 3.4$ LBGs in the PSS0808+5215 field. Objects are binned with $\Delta z = 0.03$. The redshifts of the two known DLAs are indicated by the vertical dashed lines

Cooke et al. 2006

Observational Strategy

The Detection of emissions from DLA host-galaxies at HIGH Z

(e.g. **Moller,Fynbo, Ledoux's works)**

'Large Observatories Joint Comprehensive Search'

「どのような観点からどのような観測量に注目するか」
を吟味しなければならない！

[The Aim of this Strategy]

- **The nature of high-z DLAs （金属量の切り口で）**
- **Lyman Break Galaxies （空間相関の切り口で）**
- **The hosts of Gamma-ray Bursts （吸収線プロファイルの切り口で）**

→ *モデルの予測が必要な側面がある*

Strategy for detecting emission lines from DLA galaxies at high z

(Moller 2004 private communication)

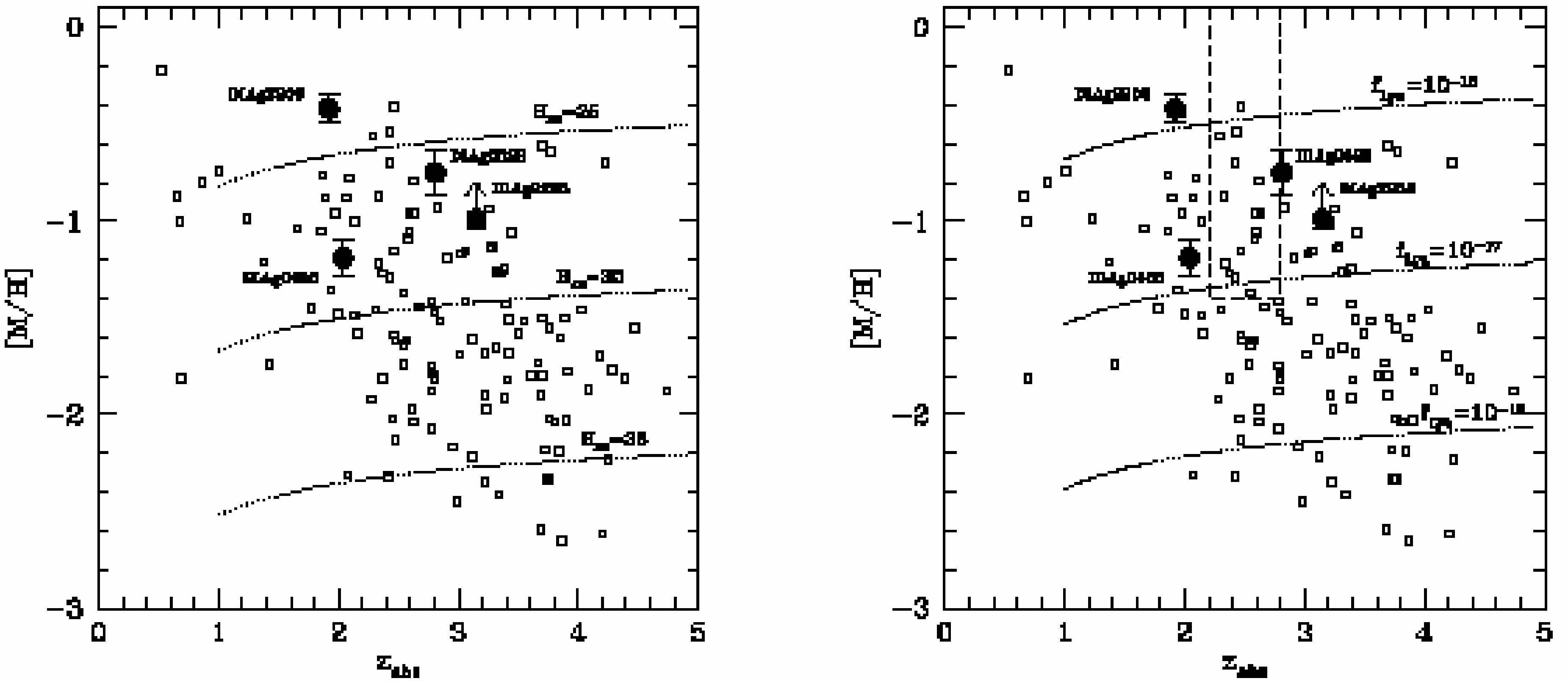

Luminous galaxies ⇒ High metallicity Z

Ly α Flux vs Metallicity relation predicted by our model

DLA galaxies (Moller et al.) (*blue dots*)
Detection limits of Subaru Telescopes (*red-dashed lines*)

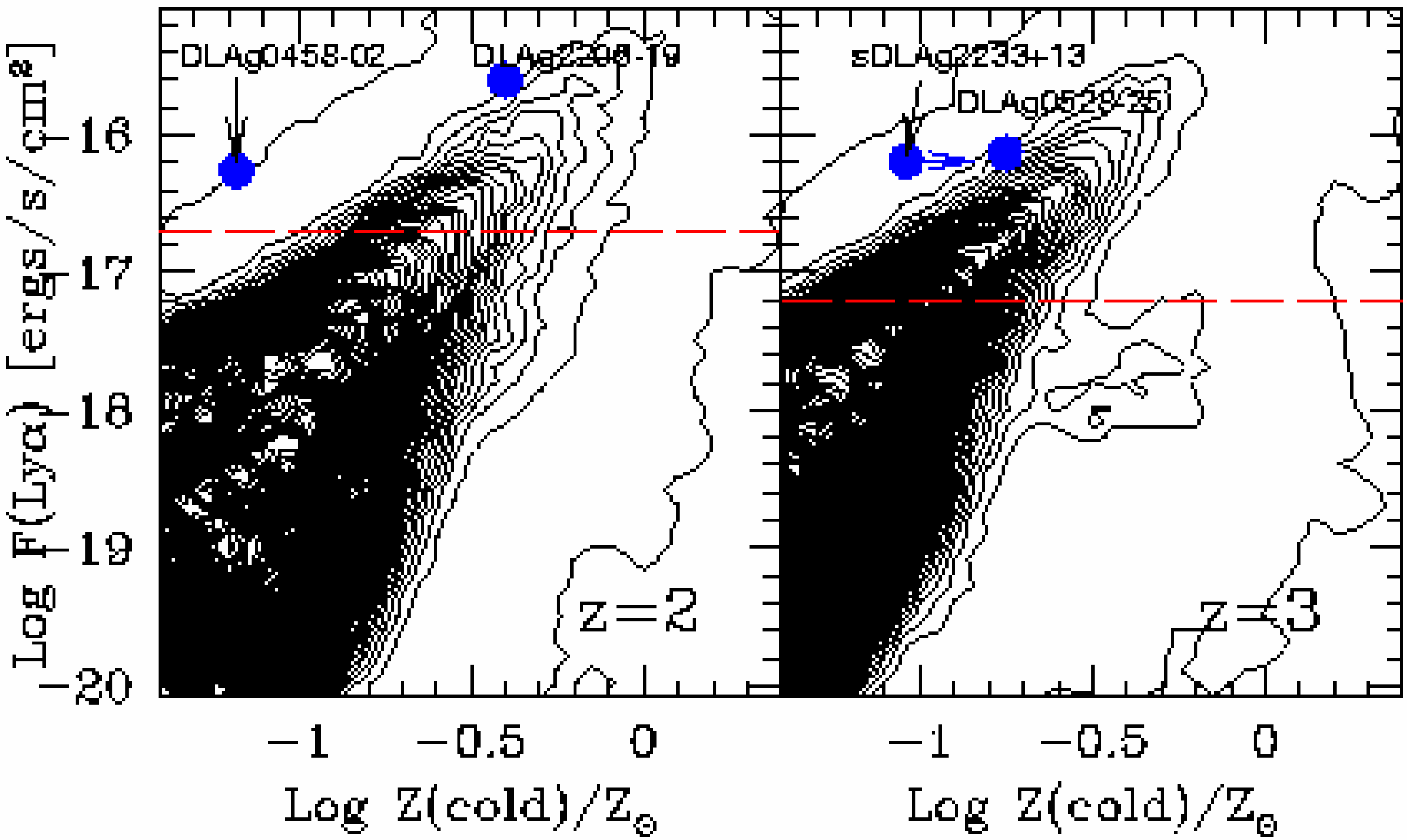

Okoshi, Minowa, Moller, Fynbo, Ledoux、Bouche et al. 2005-2006

Key points

- ***Low redshift z=0:***

  HI-selected galaxies at M(HI) <$10^8 M_\odot$

  ➡ **The nature of DLAs and subDLAs**

  ➡ **Star formation laws**

- ***High redshift z>2:***

  ➡ **Large samples !!(e.g., Spectra of GRB afterglow)**

  ➡ **Metalの空間分布 （e.g., SNe explosions)**
  Metal systems (e.g., MgII, CIV systems)
  Lyman-break galaxiesとの相関
  Sub-structure problems
  UV background radiation (Proximity effects)
  He II reionization
  Angular-momentum problems　etc…..